# Unstructured Adiabatic Quantum Optimization

Thesis submitted in partial fulfillment
of the requirements for the degree of

*Master of Science in Computer Science and Engineering by Research*

by

Alapan Chaudhuri
2019111023
alapan.chaudhuri@research.iiit.ac.in


Centre for Quantum Science and Technology (CQST)
International Institute of Information Technology (IIIT)
Hyderabad - 500032, India
February 2026

International Institute of Information Technology
Hyderabad, India

# CERTIFICATE

It is certified that the work contained in this thesis, titled "Unstructured Adiabatic Quantum Optimization" by Alapan Chaudhuri, has been carried out under my supervision and is not submitted elsewhere for a degree.

_____ _____

Date Adviser: Prof. Indranil Chakrabarty

_____ _____

Date Co-Adviser: Prof. Shantanav Chakraborty

To a world that feels like it's splitting apart.
May we keep repairing what we can.

“Computers are more forgiving than bare-bone nature or mathematics
— both of which are infinitely more forgiving than academia."

# Abstract

[TODO]

# Acknowledgement

# Contents

# List of Theorems

# List of Algorithms

# List of Figures

# Chapter 1

# Introduction

# Chapter 2

# Physics and Computation

# Chapter 3

# Quantum Computation

Chapter 4

# Adiabatic Quantum Computation

# Chapter 5

# Adiabatic Quantum Optimization

The adiabatic version of Grover's algorithm, due to Roland and Cerf [1], finds a single marked item among $N = 2^n$ by slowly interpolating between a uniform superposition and a problem Hamiltonian that penalizes all unmarked items. The crossing between the two lowest energy levels occurs at $s = 1/2$, its position independent of the Hamiltonian's spectrum. The minimum spectral gap scales as $1/\sqrt{N}$, and a schedule that slows near the crossing achieves the optimal $O(\sqrt{N})$ runtime.

Consider a cost function encoded in an $n$-qubit Hamiltonian diagonal in the computational basis, with $M$ distinct energy levels, arbitrary degeneracies, and a spectral gap that may vary with the number of qubits. The ground states encode solutions to a combinatorial optimization problem. Can the adiabatic approach still match the $\Theta(\sqrt{N})$ lower bound for unstructured search [2]? Partial answers exist: Žnidarič and Horvat [3] showed via analytical and heuristic arguments that the minimum gap scales as $\sqrt{d_0/2^n}$ for 3-SAT instances and identified the crossing position, but did not rigorously bound the runtime. Hen [4] proved a quadratic speedup for a random Hamiltonian whose energy distribution ensures a crossing position independent of the spectrum, avoiding the central difficulty.

The answer in full generality is yes, but with complications that do not arise in the single-marked-item case. The spectrum of the interpolated Hamiltonian is far richer: instead of a two-level system plus a degenerate bulk, there are $M$ interacting energy levels in a symmetric subspace, with avoided crossings between higher excited states that obscure the gap between the two lowest. The position of the ground-state avoided crossing depends nontrivially on the degeneracy structure of the problem Hamiltonian. And the minimum gap, while still scaling as $\Theta(1/\sqrt{N})$ up to spectral factors, occurs at a position that must be known to exponential precision for the schedule to be correct.

This chapter builds the framework for analyzing adiabatic quantum optimization with general diagonal Hamiltonians. We define the problem Hamiltonian and the interpolation, identify the spectral parameters that govern the crossing, reduce the $N$-dimensional eigenvalue problem to $M$ dimensions, derive the eigenvalue equation, and locate the avoided crossing with its minimum gap. The next three chapters use this framework: Chapter 6 bounds the spectral gap across the full adiabatic path, Chapter 7 derives the optimal runtime, and Chapter 8 proves that computing the crossing position is NP-hard.

## 5.1 The Problem

Consider an $n$-qubit Hamiltonian $H_z$ that is diagonal in the computational basis:

$$H_z = \sum_{z \in \{0,1\}^n} E_z \left|z\right\rangle \left\langle z\right|, \tag{5.1.1}$$

where $E_z$ is the energy assigned to bit-string $z$. Since $H_z$ acts diagonally, it encodes a classical cost function: the energy $E_z$ is the cost of configuration $z$, and the ground states are the optimal solutions. Without loss of generality, we rescale and shift so that all eigenvalues lie in $[0, 1]$.

Suppose $H_z$ has $M$ distinct energy levels with eigenvalues

$$0 \leq E_0 < E_1 < \cdots < E_{M-1} \leq 1. \tag{5.1.2}$$

For each level $k$, the set of bit-strings at that energy is

$$\Omega_k = \{z \in \{0,1\}^n : H_z \left|z\right\rangle = E_k \left|z\right\rangle\}, \tag{5.1.3}$$

with degeneracy $d_k = |\Omega_k|$. The degeneracies partition the full Hilbert space: $\sum_{k=0}^{M-1} d_k = 2^n = N$. The spectral gap of the problem Hamiltonian is $\Delta = E_1 - E_0$, the energy difference between the ground state and the first excited level.

A concrete and important instance is the 2-local Ising Hamiltonian

$$H_\sigma = \sum_{\langle i,j \rangle} J_{ij} \sigma_z^i \sigma_z^j + \sum_{j=1}^{n} h_j \sigma_z^j, \tag{5.1.4}$$

where $J_{ij}, h_j \in \{-m, -m+1, \ldots, m\}$ for some constant positive integer $m$. After normalization, $H_\sigma$ has $M \in \text{poly}(n)$ distinct eigenvalues and a spectral gap $\Delta \geq 1/\text{poly}(n)$. Solutions to NP-hard problems such as MaxCut and QUBO encode directly in the ground states of $H_\sigma$ with minimal overhead [5, 6].

For the running example, take unstructured search: $M = 2$ energy levels, a single ground state ($d_0 = 1$) with energy $E_0 = 0$, and $N - 1$ excited states ($d_1 = N - 1$) at energy $E_1 = 1$. The ground state is the "marked item." Classical search requires $\Theta(N)$ queries; Grover's circuit algorithm requires $\Theta(\sqrt{N})$ [7, 8].

To solve this optimization problem adiabatically, we interpolate between an initial Hamiltonian whose ground state is easy to prepare and the problem Hamiltonian whose ground state encodes the solution. The initial Hamiltonian is the rank-one projector

$$H_0 = -|\psi_0\rangle\langle\psi_0|, \qquad |\psi_0\rangle = |+\rangle^{\otimes n} = \frac{1}{\sqrt{N}} \sum_{z \in \{0,1\}^n} |z\rangle. \tag{5.1.5}$$

Every computational basis state receives equal amplitude, so $|\psi_0\rangle$ introduces no bias toward any particular solution.

The adiabatic Hamiltonian is the linear interpolation

$$H(s) = -(1-s)|\psi_0\rangle\langle\psi_0| + sH_z, \qquad s \in [0,1]. \tag{5.1.6}$$

At $s = 0$, the ground state is $|\psi_0\rangle$ with energy $-1$, and all other states have energy 0. At $s = 1$, the Hamiltonian is $H_z$ itself, and its ground states encode the solutions. The adiabatic theorem guarantees that if the schedule $s(t)$ traverses $[0,1]$ slowly enough, the evolved state remains close to the instantaneous ground state throughout, arriving at the end in a state with high overlap with the ground space of $H_z$.

The choice of a rank-one projector for $H_0$, rather than a more general Hamiltonian, has a structural consequence. At $s = 0$, the spectrum of $H(s)$ has a single non-degenerate eigenvalue at $-1$ (the ground state) and an $(N-1)$-fold degenerate eigenvalue at 0. As $s$ increases, the degeneracy splits according to the spectrum of $H_z$, but the ground state can only interact with one effective excited state at a time. This produces a single avoided crossing between the two lowest energy levels, in contrast to generic AQC Hamiltonians that may exhibit multiple crossings requiring different analytical techniques [9]. The single-crossing structure is what makes a complete spectral analysis tractable.

For the running example, $H(s) = -(1-s)|\psi_0\rangle\langle\psi_0| + s(I - |w\rangle\langle w|)$, where $|w\rangle$ is the marked item. Up to a global energy shift of $s$, this is the Roland-Cerf Hamiltonian [1]. The spectrum has $N - 2$ states at energy $s$ (degenerate, orthogonal to both $|\psi_0\rangle$ and $|w\rangle$) and two states whose energies depend on $s$ and undergo an avoided crossing near $s = 1/2$.

## 5.2 Spectral Parameters

In the Roland-Cerf setting, the crossing position ($s^* = 1/2$), its width, and the minimum gap are all determined by a single quantity: $N$. For a general problem Hamiltonian $H_z$ with $M$ energy levels and arbitrary degeneracies, no single number suffices. The relevant information is captured by a family of spectral parameters that aggregate the degeneracy structure weighted by inverse energy gaps.

**Definition 5.2.1** (Spectral parameters)**.** *For the problem Hamiltonian $H_z$ with eigenvalues $E_0 < E_1 < \cdots < E_{M-1}$ and degeneracies $d_k$, define*

$$A_p = \frac{1}{N} \sum_{k=1}^{M-1} \frac{d_k}{(E_k - E_0)^p}, \qquad p \in \mathbb{N}. \tag{5.2.1}$$

Each excited level contributes its degeneracy $d_k$ weighted by the inverse $p$-th power of its distance to the ground energy. Higher values of $p$ emphasize levels closer to the ground state. The normalization by $N = 2^n$ makes $A_p$ an average over the full Hilbert space.

For the running example ($M = 2$, $d_0 = 1$, $d_1 = N - 1$, $E_0 = 0$, $E_1 = 1$):

$$A_p = \frac{N-1}{N} \approx 1 \quad \text{for all } p, \tag{5.2.2}$$

since $E_1 - E_0 = 1$. The spectral parameters are trivial in this case, which is precisely why the Roland-Cerf analysis is simple.

For a general Ising Hamiltonian with $\Delta \geq 1/\text{poly}(n)$ and $M \in \text{poly}(n)$, the bound $A_1 \leq (1 - d_0/N)/\Delta$ gives $A_1 = O(\text{poly}(n))$, while $A_2 \geq 1 - d_0/N$ ensures $A_2 = \Theta(1)$ at minimum.

The first two parameters play distinct roles that will become precise in subsequent sections. The parameter $A_1$ determines the position of the avoided crossing: $s^* = A_1/(A_1 + 1)$. The parameter $A_2$ enters the minimum spectral gap: $g_{\min} = \Theta(\sqrt{d_0/(NA_2)})$. Both appear in the runtime: $T = O((\sqrt{A_2}/A_1^2\Delta^2)\sqrt{N/d_0})$.

Since every eigenvalue gap satisfies $E_k - E_0 \leq 1$ and the total excited degeneracy is $\sum_{k\geq 1} d_k = N - d_0$, we have

$$A_2 \geq \frac{1}{N}\sum_{k=1}^{M-1} d_k = 1 - \frac{d_0}{N}. \tag{5.2.3}$$

For $d_0 \ll N$ (few solutions), $A_2 \geq 1 - 1/N$ is close to 1. Also, $A_1 \leq (1 - d_0/N)/\Delta$, since $(E_k - E_0)^{-1} \leq \Delta^{-1}$ for all $k \geq 1$. Since $E_k - E_0 \geq \Delta$ for all $k \geq 1$, termwise comparison gives $A_1 \geq A_2\Delta$. Since $E_k - E_0 \leq 1$, we also have $A_1 \leq A_2$. Together: $A_2\Delta \leq A_1 \leq A_2$.

The behavior of the adiabatic Hamiltonian is well-controlled only when the avoided crossing region is narrow compared to the interval $[0, 1]$. This is ensured by a spectral condition on $H_z$.

**Definition 5.2.2** (Spectral condition)**.** *The problem Hamiltonian $H_z$ satisfies the spectral condition if there exists a constant $c \ll 1$ such that*

$$\frac{1}{\Delta}\sqrt{\frac{d_0}{A_2 N}} < c. \tag{5.2.4}$$

The quantity on the left is the ratio of the crossing width parameter to the spectral gap, up to constant factors. When it is small, the two-level approximation near the crossing is accurate (the higher levels do not interfere), and the crossing window occupies a negligible fraction of $[0, 1]$. The appendix of the published paper shows that $c \approx 0.02$ suffices [10].

For any $H_z$ with $\Delta > (1/c)\sqrt{d_0/N}$, the condition holds, using $A_2 \geq 1 - d_0/N$. For the Ising Hamiltonian with $\Delta \geq 1/\text{poly}(n)$ and $d_0$ not scaling with $N$, the left side is exponentially small in $n$, so the condition is easily satisfied. For the running example with $\Delta = 1$ and $d_0 = 1$, the left side is $1/\sqrt{N}$, well below any constant $c$ for $N \geq 2$.

## 5.3 Symmetry Reduction

The Hilbert space of $H(s)$ has dimension $N = 2^n$, exponentially large in the number of qubits. Direct spectral analysis is intractable. But the problem Hamiltonian $H_z$ has only $M$ distinct energy levels, and the initial state $|\psi_0\rangle$ treats all bit-strings at the same energy identically. This permutation symmetry within each degenerate subspace reduces the eigenvalue problem from $N$ dimensions to $M$.

For each energy level $k$, define the symmetric state

$$|k\rangle = \frac{1}{\sqrt{d_k}}\sum_{z\in\Omega_k} |z\rangle\,, \qquad 0 \leq k \leq M-1. \tag{5.3.1}$$

These $M$ states are orthonormal: $\langle j\rangle\, k = \delta_{jk}$. They span the $M$-dimensional symmetric subspace

$$\mathcal{H}_S = \text{span}\,\{|k\rangle : 0 \leq k \leq M-1\}\,. \tag{5.3.2}$$

In this basis, the problem Hamiltonian has $M$ non-degenerate eigenvalues:

$$H_z = \sum_{k=0}^{M-1} E_k\,|k\rangle\langle k| \quad \text{on } \mathcal{H}_S, \tag{5.3.3}$$

and the initial state decomposes as

$$|\psi_0\rangle = \sum_{k=0}^{M-1}\sqrt{\frac{d_k}{N}}\,|k\rangle\,. \tag{5.3.4}$$

Since $|\psi_0\rangle \in \mathcal{H}_S$ and both $H_z$ and $|\psi_0\rangle\langle\psi_0|$ map $\mathcal{H}_S$ to itself, the adiabatic Hamiltonian $H(s)$ leaves $\mathcal{H}_S$ invariant. The time evolution starting from $|\psi_0\rangle$ remains in $\mathcal{H}_S$ for all $s$.

The complement $\mathcal{H}_S^\perp$ has dimension $N-M$ and is spanned by states orthogonal to $|\psi_0\rangle$ within each degenerate subspace. For each level $k$, order the bit-strings in $\Omega_k$ as $z_k^{(1)}, \ldots, z_k^{(d_k)}$ and define the Fourier basis

$$|k^{(\ell)}\rangle = \frac{1}{\sqrt{d_k}} \sum_{\ell'=1}^{d_k} \exp\left[\frac{i2\pi\ell\ell'}{d_k}\right] |z_k^{(\ell')}\rangle\,, \qquad 1 \le \ell \le d_k - 1. \tag{5.3.5}$$

Note that $|k^{(0)}\rangle = |k\rangle$ is the symmetric state already in $\mathcal{H}_S$. The remaining $d_k - 1$ states for each level $k$ form a basis for $\mathcal{H}_S^\perp$:

$$\mathcal{H}_S^\perp = \text{span}\left\{|k^{(\ell)}\rangle : 0 \le k \le M-1,\ 1 \le \ell \le d_k - 1\right\}. \tag{5.3.6}$$

Each $|k^{(\ell)}\rangle$ is an eigenstate of $H(s)$ with eigenvalue $sE_k$:

$$H(s)\,|k^{(\ell)}\rangle = -(1-s)\,|\psi_0\rangle \underbrace{\langle\psi_0|\,k^{(\ell)}\rangle}_{=0} + sE_k\,|k^{(\ell)}\rangle = sE_k\,|k^{(\ell)}\rangle\,. \tag{5.3.7}$$

The inner product vanishes because $|k^{(\ell)}\rangle$ is orthogonal to $|k\rangle = |k^{(0)}\rangle$ by construction, and $|\psi_0\rangle$ is a linear combination of the $|k\rangle$ states. These $N - M$ eigenstates are spectators: their eigenvalues $sE_k$ are trivially known and they do not participate in the adiabatic evolution.

Henceforth, $H(s)$ denotes its restriction to the symmetric subspace $\mathcal{H}_S$:

$$H(s) = -(1-s)\,|\psi_0\rangle\langle\psi_0| + s\sum_{k=0}^{M-1} E_k\,|k\rangle\langle k|\,. \tag{5.3.8}$$

This is a rank-one perturbation of the diagonal matrix $sH_z$. Its eigenvalues can be characterized exactly.

**Lemma 5.3.1** (Eigenvalue equation)**.** *Let $H(s)$ be the adiabatic Hamiltonian restricted to $\mathcal{H}_S$ as in Eq. (5.3.8). Then $\lambda(s)$ is an eigenvalue of $H(s)$ if and only if*

$$\frac{1}{1-s} = \frac{1}{N}\sum_{k=0}^{M-1} \frac{d_k}{sE_k - \lambda(s)}. \tag{5.3.9}$$

*Proof.* Let $|\psi\rangle = \sum_{k=0}^{M-1} \alpha_k\,|k\rangle$ be an eigenstate of $H(s)$ with eigenvalue $\lambda$, and set $\gamma = \langle\psi_0|\,\psi\rangle$. Acting with $H(s)$ on $|\psi\rangle$:

$$H(s)\,|\psi\rangle = s\sum_{k=0}^{M-1} E_k\alpha_k\,|k\rangle - (1-s)\gamma\,|\psi_0\rangle = \lambda\sum_{k=0}^{M-1}\alpha_k\,|k\rangle\,. \tag{5.3.10}$$

Comparing coefficients of $|k\rangle$ and using $\langle\psi_0|\,k\rangle = \sqrt{d_k/N}$ gives

$$\alpha_k = \frac{(1-s)\gamma\sqrt{d_k/N}}{sE_k - \lambda}. \tag{5.3.11}$$

Since $\gamma = \langle\psi_0|\,\psi\rangle = (1/\sqrt{N})\sum_k \alpha_k\sqrt{d_k}$, substituting Eq. (5.3.11) yields

$$1 = \frac{1-s}{N}\sum_{k=0}^{M-1}\frac{d_k}{sE_k - \lambda}, \tag{5.3.12}$$

which is equivalent to Eq. (5.3.9). Each step is reversible: given a solution $\lambda$ of Eq. (5.3.9), the coefficients in Eq. (5.3.11) define an eigenstate (after normalization), provided $\gamma \neq 0$. The case $\gamma = 0$ corresponds to $\lambda = sE_k$ for some $k$, which are the eigenvalues in $\mathcal{H}_S^\perp$ already accounted for. □

The right-hand side of Eq. (5.3.9), viewed as a function of $\lambda$, is a sum of $M$ terms, each a decreasing function with a vertical asymptote at $\lambda = sE_k$. Between consecutive poles $sE_{k-1}$ and $sE_k$, the function decreases monotonically from $+\infty$ to $-\infty$, producing exactly one root per interval. Below the lowest pole $sE_0$, there is one additional root. The total count is $M$ eigenvalues in $\mathcal{H}_S$, consistent with the dimension.

The two lowest eigenvalues are $\lambda_0(s) < sE_0$ (ground state) and $\lambda_1(s) \in (sE_0, sE_1)$ (first excited state). The spectral gap is $g(s) = \lambda_1(s) - \lambda_0(s) > 0$. However, the eigenvalue equation alone gives only the trivial bound

$0 < g(s) < s\Delta$, since $\lambda_0(s)$ could be arbitrarily close to $sE_0$ from below while $\lambda_1(s)$ could be close to $sE_0$ from above. Extracting tight bounds requires analyzing the eigenvalue equation in the vicinity of the crossing.

For the running example ($M = 2$), Eq. (5.3.9) becomes

$$\frac{1}{1-s} = \frac{1}{N} \cdot \frac{1}{-\lambda} + \frac{N-1}{N} \cdot \frac{1}{s-\lambda}, \tag{5.3.13}$$

where we set $E_0 = 0$ and $E_1 = 1$. Clearing denominators produces the quadratic $N\lambda^2 - N(2s-1)\lambda - s(1-s) = 0$, whose two roots give the ground and first excited energies:

$$\lambda_\pm(s) = \frac{2s-1}{2} \pm \frac{1}{2}\sqrt{(2s-1)^2 + \frac{4s(1-s)}{N}}. \tag{5.3.14}$$

At $s = 0$, the ground energy is $\lambda_- = -1$ and the first excited energy is $\lambda_+ = 0$, consistent with the spectrum of $H(0) = -|\psi_0\rangle\langle\psi_0|$. The gap $g(s) = \lambda_+(s) - \lambda_-(s)$ simplifies to

$$g(s) = \sqrt{(2s-1)^2 + \frac{4s(1-s)}{N}}, \tag{5.3.15}$$

which is minimized at $s = 1/2$ exactly, giving $g_{\min} = 1/\sqrt{N}$. This is the Roland-Cerf gap. The general theory of the next section reproduces this scaling as a special case.

## 5.4 The Avoided Crossing

The eigenvalue equation (Lemma 5.3.1) characterizes the spectrum of $H(s)$ implicitly. We now extract explicit formulas for the crossing position, its width, and the minimum gap by analyzing the equation near the ground state energy. Near the crossing, the ground and first excited states behave like a two-level system, with the higher levels acting as a perturbation controlled by the spectral condition.

The two lowest eigenvalues have the form $\lambda(s) = sE_0 + \delta(s)$, where $\delta(s)$ is a correction to the trivial energy $sE_0$. Substituting into Eq. (5.3.9) [11]:

$$-\frac{d_0}{N\delta} + \frac{1}{N}\sum_{k=1}^{M-1} \frac{d_k}{s(E_k - E_0) - \delta} = \frac{1}{1-s}. \tag{5.4.1}$$

The first term has a pole at $\delta = 0$; the sum has poles at $\delta = s(E_k - E_0)$ for $k \geq 1$. When $|\delta| \ll s\Delta$ (guaranteed by the spectral condition), the sum can be expanded in powers of $\delta/(s(E_k - E_0))$:

$$\frac{1}{N}\sum_{k=1}^{M-1} \frac{d_k}{s(E_k - E_0) - \delta} = \frac{1}{s}\left(A_1 + \frac{\delta}{s}A_2 + \frac{\delta^2}{s^2}A_3 + \cdots\right). \tag{5.4.2}$$

Truncating at the $A_2$ term and rearranging Eq. (5.4.1) gives a quadratic in $\delta$ whose two roots are the corrections $\delta_0^+(s)$ and $\delta_0^-(s)$ for the first excited and ground states, respectively:

$$\delta_0^\pm(s) = \frac{s(A_1+1)}{2A_2(1-s)}\left[(s-s^*) \pm \sqrt{(s^*-s)^2 + \frac{4A_2 d_0}{N(A_1+1)^2}(1-s)^2}\right], \tag{5.4.3}$$

Here $\delta_0^+(s) > 0$ corresponds to the first excited state and $\delta_0^-(s) < 0$ to the ground state: the superscript indicates the sign of the correction relative to $sE_0$. The crossing position is

$$s^* = \frac{A_1}{A_1 + 1}. \tag{5.4.4}$$

The quantity $s^*$ is the position of the avoided crossing. It is entirely determined by $A_1$, and hence by the degeneracy-weighted inverse gaps of the problem Hamiltonian. For the Ising Hamiltonian with $\Delta \geq 1/\text{poly}(n)$, we have $A_1 \geq \Theta(1)$, so $s^*$ is bounded away from both 0 and 1. In the limit $A_1 \to \infty$ (many levels near the ground state), $s^* \to 1$; when $A_1$ is small, $s^*$ is closer to 0.

The crossing position marks a balance in the eigenvalue equation: $A_1/s^* = 1/(1-s^*)$, where the left side is the aggregate spectral pull of the excited levels toward $sE_0$ and the right side is the projector strength. At $s = s^*$, the linear coefficient in the quadratic for $\delta$ (Eq. (5.4.3)) vanishes, and the two roots $\delta_0^\pm$ are symmetric

about zero. The gap is determined entirely by the constant term $d_0/N$: the ground-state degeneracy is what opens the minimum gap.

The truncation is an approximation. The actual roots $\delta_\pm(s)$ of the full equation differ from $\delta_0^\pm(s)$ by a relative error controlled by the spectral condition. The following result, whose proof uses the intermediate value theorem on the full equation after bounding the remainder using $A_3$ and the spectral condition, makes this precise [10, 12].

**Lemma 5.4.1** (Validity of approximation)**.** *Let $H_z$ satisfy the spectral condition (Definition 5.2.2) with constant $c \approx 0.02$, and define*

$$\delta_s = \frac{2}{(A_1+1)^2}\sqrt{\frac{d_0 A_2}{N}}. \tag{5.4.5}$$

*Then for any $s \in \mathcal{I}_{s^*} = [s^* - \delta_s,\ s^* + \delta_s]$, there exists a constant $\eta \ll 1$ such that the two lowest eigenvalues of $H(s)$ satisfy*

$$\delta_+(s) \in \left((1-\eta)\,\delta_0^+(s),\ (1+\eta)\,\delta_0^+(s)\right), \tag{5.4.6}$$

$$\delta_-(s) \in \left((1+\eta)\,\delta_0^-(s),\ (1-\eta)\,\delta_0^-(s)\right), \tag{5.4.7}$$

*where $\delta_0^\pm(s)$ are given by Eq. (5.4.3).*

The proof evaluates the full equation (5.4.1) at $\delta_0^\pm(1\pm\eta)$ and shows, using the spectral condition to bound the truncated Taylor remainder, that the full equation changes sign between these points. The intermediate value theorem then guarantees a root in the interval. The spectral condition enters through the bound $|\delta_0^\pm(s)|/(s\Delta) \le \kappa c < 1$, where $\kappa$ is a constant depending on $c$, ensuring the geometric series in the Taylor expansion converges. The constant $c \approx 0.02$ is sufficient for $\eta \le 0.1$. The complete calculation appears in the appendix of the published paper [10].

The spectral gap $g(s) = \delta_+(s) - \delta_-(s)$ is therefore approximated to within a factor of $1\pm 2\eta$ by $\delta_0^+(s) - \delta_0^-(s)$, which evaluates to

$$g(s) = (1 \pm 2\eta)\cdot \frac{s(A_1+1)}{A_2(1-s)}\sqrt{(s^*-s)^2 + \frac{4A_2 d_0}{N(A_1+1)^2}(1-s)^2}. \tag{5.4.8}$$

At $s = s^*$, the first term under the square root vanishes, leaving only the second:

$$g_{\min} = g(s^*) \ge (1-2\eta)\cdot \frac{2A_1}{A_1+1}\sqrt{\frac{d_0}{NA_2}}. \tag{5.4.9}$$

This is the minimum spectral gap of $H(s)$.

The formulas decompose as follows. The factor $2A_1/(A_1+1)$ captures the position of the crossing: a crossing near the boundary ($s^* \to 0$ or $s^* \to 1$) reduces the gap. The factor $\sqrt{d_0/N}$ is the Grover-like contribution: more solutions (larger $d_0$) increase the gap and reduce the runtime. The factor $1/\sqrt{A_2}$ encodes the spectral structure beyond the simplest two-level case.

The crossing position $s^*$, the window width $\delta_s$, and the leading-order minimum gap are connected by an exact algebraic identity. Writing $\hat{g} = \frac{2A_1}{A_1+1}\sqrt{\frac{d_0}{NA_2}}$ for the leading-order expression, direct substitution gives

$$\frac{s^*(A_1+1)^2}{A_2}\cdot \delta_s = \hat{g}, \tag{5.4.10}$$

and by Eq. (5.4.9), $g_{\min} \ge (1-2\eta)\hat{g}$. This relation will be used in Chapter 7 to verify the runtime calculation.

The interval $[0,1]$ splits into three regions based on the crossing:

$$\mathcal{I}_{s^\leftarrow} = [0,\ s^* - \delta_s), \qquad \mathcal{I}_{s^*} = [s^* - \delta_s,\ s^* + \delta_s], \qquad \mathcal{I}_{s^\rightarrow} = (s^* + \delta_s,\ 1]. \tag{5.4.11}$$

Within the window $\mathcal{I}_{s^*}$, the gap is bounded both from below and above in terms of $g_{\min}$.

**Lemma 5.4.2** (Gap within the crossing window)**.** *Let $H_z$ satisfy the spectral condition with constant $c$, and define*

$$\kappa' = \frac{(1+2\eta)(1+2c)}{(1-2\eta)(1-2c)}\sqrt{1+(1-2c)^2}. \tag{5.4.12}$$

*Then for any $s \in \mathcal{I}_{s^*}$,*

$$g_{\min} \le g(s) \le \kappa' \cdot g_{\min}. \tag{5.4.13}$$

*Proof.* The lower bound is immediate from the definition of $g_{\min}$ as the minimum over $\mathcal{I}_{s^*}$. For the upper bound, start from Eq. (5.4.8) with $|s - s^*| \le \delta_s$:

$$g(s) \le \frac{s(A_1+1)}{A_2(1-s)}\sqrt{\delta_s^2 + \frac{4A_2 d_0}{N(A_1+1)^2}(1-s)^2}. \tag{5.4.14}$$

Factoring out $(A_1+1)\delta_s(1-s)$ under the square root and using $s/s^* \le 1 + \delta_s/s^*$:

$$g(s) \le \frac{s^*(A_1+1)^2}{A_2}\delta_s \cdot \frac{s}{s^*} \cdot \sqrt{\frac{1}{(1-s)^2(A_1+1)^2} + 1}. \tag{5.4.15}$$

The first factor equals $\hat{g}$ by Eq. (5.4.10). The spectral condition gives $\delta_s/(1-s^*) \le 2c$ and $\delta_s/s^* \le 2c$. To see the first, compute

$$\frac{\delta_s}{1-s^*} = \frac{2}{1+A_1}\sqrt{\frac{d_0 A_2}{N}} = \frac{2A_2\Delta}{1+A_1}\cdot\frac{1}{\Delta}\sqrt{\frac{d_0}{A_2 N}} \le 2s^* c \le 2c, \tag{5.4.16}$$

where we used $A_2\Delta/(1+A_1) \le A_1/(1+A_1) = s^*$. The bound $\delta_s/s^* \le 2c$ follows similarly. Substituting into the upper bound:

$$g(s) \le (1+2\eta)\hat{g}\cdot(1+2c)\sqrt{1+(1-2c)^2} \le \kappa' \cdot g_{\min}, \tag{5.4.17}$$

where the factor $(1+2\eta)$ comes from the upper approximation in Eq. (5.4.8), and the last step uses $\hat{g} \le g_{\min}/(1-2\eta)$. □

The spectral gap is therefore of order $g_{\min}$ throughout $\mathcal{I}_{s^*}$ and strictly larger outside this window, as the next section establishes. The avoided crossing is localized.

For the running example, the formulas specialize cleanly. With $A_1 = A_2 = (N-1)/N$:

$$s^* = \frac{(N-1)/N}{(N-1)/N+1} = \frac{N-1}{2N-1} \approx \frac{1}{2}, \tag{5.4.18}$$

$$g_{\min} = \frac{2(N-1)/(2N-1)}{\sqrt{N\cdot(N-1)/N}} = \frac{2(N-1)}{(2N-1)\sqrt{N-1}} \approx \frac{1}{\sqrt{N}}, \tag{5.4.19}$$

$$\delta_s = \frac{2N^2}{(2N-1)^2}\sqrt{\frac{N-1}{N^2}} \approx \frac{1}{2\sqrt{N}}. \tag{5.4.20}$$

The crossing is at $s^* \approx 1/2$, the minimum gap scales as $1/\sqrt{N}$, and the window width scales as $1/\sqrt{N}$. These agree asymptotically with the exact quadratic solution in Eq. (5.3.15), confirming the general theory reproduces the known scaling. The small discrepancy between $s^* = (N-1)/(2N-1)$ and the exact minimum at $s = 1/2$ is a higher-order effect of the two-level truncation, vanishing as $O(1/N)$.

## 5.5 Gap Structure

The previous section characterized the spectral gap within the crossing window $\mathcal{I}_{s^*}$: it is $\Theta(g_{\min})$ throughout. For the adiabatic algorithm, we also need the gap outside this window. The local adaptive schedule that achieves optimal runtime requires knowing how the gap grows as $s$ moves away from $s^*$, so that the evolution speeds up in regions of larger gap.

The following two results, proved in Chapter 6, bound the gap in the left and right regions.

**Lemma 5.5.1** (Gap to the left of the crossing)**.** *For any $s \in \mathcal{I}_{s^*} = [0,\, s^* - \delta_s)$, the spectral gap of $H(s)$ satisfies*

$$g(s) \ge \frac{A_1(A_1+1)}{A_2}(s^* - s). \tag{5.5.1}$$

The proof, detailed in Chapter 6, uses the variational principle: an explicit ansatz $|\phi\rangle$ provides an upper bound on the ground energy $\lambda_0(s) \le \langle\phi|\, H(s)\, |\phi\rangle$, while the eigenvalue equation gives the lower bound $\lambda_1(s) \ge sE_0$ on the first excited energy. The ansatz is

$$|\phi\rangle = \frac{1}{\sqrt{A_2 N}}\sum_{k=1}^{M-1}\frac{\sqrt{d_k}}{E_k - E_0}\,|k\rangle\,, \tag{5.5.2}$$

which concentrates amplitude on levels close to the ground energy, yielding a tight upper bound on $\lambda_0(s)$. A second route uses concavity: since $\lambda_0(s) = \min_{|\psi\rangle}\langle\psi|\, H(s)\, |\psi\rangle$ is the pointwise minimum of functions linear in $s$, it is concave. The tangent to a concave function lies above it, so the tangent to $\lambda_0$ at $s^*$ gives a linear upper bound that, combined with $\lambda_1(s) \ge sE_0$, reproduces Eq. (5.5.1). Chapter 6 develops both approaches.

**Lemma 5.5.2** (Gap to the right of the crossing)**.** *Let $k = 1/4$, $a = 4k^2\Delta/3$, and*

$$s_0 = s^* - \frac{k\, g_{\min}(1 - s^*)}{a - k\, g_{\min}}. \tag{5.5.3}$$

*Then for all $s \geq s^*$, the spectral gap of $H(s)$ satisfies*

$$g(s) \geq \frac{\Delta}{30} \cdot \frac{s - s_0}{1 - s_0}. \tag{5.5.4}$$

This bound is linear in $s - s_0$, with a slope proportional to $\Delta$. The proof, also in Chapter 6, uses the resolvent method: a line $\gamma(s) = sE_0 + \beta(s)$ is placed between the two lowest eigenvalues, and the Sherman-Morrison formula [13] bounds the resolvent norm $\|R_{H(s)}(\gamma)\|$, giving $g(s) \geq 2/\|R_{H(s)}(\gamma)\|$. The constants $k = 1/4$ and $a = 4k^2\Delta/3$ are tuned to make the resulting function $f(s)$ monotonically decreasing on $[s^*, 1]$, yielding the clean bound $\Delta/30$.

Both bounds exceed $g_{\min}$ at the window boundary. At $s = s^* - \delta_s$ (left boundary), the left bound gives

$$g(s^* - \delta_s) \geq \frac{A_1(A_1 + 1)}{A_2} \cdot \delta_s = \frac{2A_1}{A_1 + 1}\sqrt{\frac{d_0}{NA_2}} = \hat{g}, \tag{5.5.5}$$

which satisfies $\hat{g} \geq g_{\min}/(1 - 2\eta)$ by Eq. (5.4.9). At $s = s^*$ (right boundary start), $\beta(s^*) \geq k\, g_{\min}$, so $g(s^*) \geq 2k\, g_{\min}/(1 + f(s^*)) = O(g_{\min})$ since $f(s^*) = \Theta(1)$. The gap profile is therefore continuous across region boundaries: it dips to $g_{\min}$ at $s^*$ and rises linearly on both sides.

The complete gap profile feeds directly into the runtime calculation. The optimal local adaptive schedule has $ds/dt \propto g(s)^2$: the evolution slows quadratically as the gap decreases. The total runtime is

$$T \propto \int_0^1 \frac{ds}{g(s)^2}, \tag{5.5.6}$$

split across the three regions. In the left and right regions, the linear growth $g(s) \propto |s - s^*|$ makes $1/g(s)^2 \propto 1/(s - s^*)^2$, which integrates to a logarithmic contribution. In the window, $g(s) = \Theta(g_{\min})$ is approximately constant, giving a contribution proportional to $2\delta_s/g_{\min}^2$. The window dominates:

$$\frac{\delta_s}{g_{\min}^2} \propto \frac{\sqrt{A_2}}{A_1^2\Delta^2}\sqrt{\frac{N}{d_0}}, \tag{5.5.7}$$

yielding the runtime of Theorem 1 in the published paper [10]. For the Ising Hamiltonian with $A_1, A_2 = O(\text{poly}(n))$ and $\Delta \geq 1/\text{poly}(n)$, this gives $T = \widetilde{O}(\sqrt{N/d_0})$, matching the Grover lower bound up to polylogarithmic factors. Chapter 7 carries out this calculation rigorously.

## 5.6 The Central Questions

The framework is now complete. The adiabatic Hamiltonian $H(s)$ interpolates between the easy initial state and the problem Hamiltonian. The symmetry reduction collapses the $N$-dimensional problem to $M$ dimensions. The eigenvalue equation characterizes the spectrum implicitly, and the two-level approximation near the crossing yields explicit formulas for $s^*$, $\delta_s$, and $g_{\min}$. The gap is $\Theta(g_{\min})$ in the crossing window and grows linearly outside it.

The first question is technical: are the gap bounds in the left and right regions tight? The variational bound for the left region and the resolvent bound for the right region have been stated but not proved. Chapter 6 develops both proofs in full, including the construction of the variational ansatz, the Sherman-Morrison resolvent calculation, and the monotonicity analysis for the function $f(s)$.

The second question is the main positive result: what is the optimal runtime? The answer, derived in Chapter 7, is

$$T = O\left(\frac{1}{\varepsilon} \cdot \frac{\sqrt{A_2}}{A_1^2\Delta^2} \cdot \sqrt{\frac{N}{d_0}}\right), \tag{5.6.1}$$

where $\varepsilon$ is the target error. For Ising Hamiltonians, this is $\widetilde{O}(\sqrt{N/d_0})$, matching the lower bound of Farhi, Goldstone, and Gutmann [2]. Adiabatic quantum optimization achieves the Grover speedup.

The third question reveals the limitation. The local adaptive schedule requires knowing $s^*$ to precision $O(\delta_s) = O(2^{-n/2})$, which requires knowing $A_1$ to comparable precision. How hard is this computation? Chapter

8 proves that approximating $A_1$ to additive accuracy $1/\mathrm{poly}(n)$ is NP-hard: two queries to such an oracle suffice to solve 3-SAT. Computing $A_1$ exactly, or to accuracy $O(2^{-\mathrm{poly}(n)})$, is #P-hard: polynomial interpolation extracts all degeneracies $d_k$ from $O(\mathrm{poly}(n))$ exact queries. There is an exponential gap between the precision needed ($O(2^{-n/2})$) and the precision at which the problem is already NP-hard ($1/\mathrm{poly}(n)$).

The fourth question confronts this tension. In the circuit model, Grover's algorithm achieves $\widetilde{O}(\sqrt{N/d_0})$ without pre-computing any spectral parameter: the oracle queries gather the needed information adaptively during execution. The adiabatic framework requires the schedule to be fixed before the evolution begins, necessitating the NP-hard pre-computation. This asymmetry is not an artifact of the analysis but a genuine difference between the two computational models. The paper [10] calls this "optimality with limitations": the adiabatic speedup exists but is contingent on solving a hard problem first. Chapter 9 characterizes this information-runtime tradeoff precisely, proving a separation theorem for uninformed schedules, a smooth interpolation for partial information, and an adaptive measurement protocol that circumvents the classical hardness.

For the running example, the limitation vanishes: $A_1 = (N-1)/N \approx 1$ is trivially known, so $s^* \approx 1/2$ requires no hard computation. The complexity arises only for problem Hamiltonians with rich spectral structure, where the degeneracies $d_k$ and energy gaps $E_k - E_0$ are not known in advance. The Ising Hamiltonian encoding an NP-hard problem is precisely such a case.

# Chapter 6

# Spectral Analysis

Chapter 5 established the crossing window $\mathcal{I}_{s^*}$ where the spectral gap satisfies $g(s) = \Theta(g_{\min})$, and stated two bounds for the regions outside: a linear lower bound to the left (Lemma 5.5.1) and a linear lower bound to the right (Lemma 5.5.2). The complete gap profile determines the runtime of the adiabatic algorithm through the integral $\int_0^1 g(s)^{-2}\, ds$. This chapter proves both lemmas.

The two proofs use different techniques, reflecting different spectral structures on each side of the crossing. To the left of $s^*$, the ground energy $\lambda_0(s)$ sits below $sE_0$ while the first excited energy $\lambda_1(s)$ sits above it. The variational principle bounds how far below $sE_0$ the ground energy can be, yielding a linear gap bound. To the right of $s^*$, the eigenvalues of $sH_z$ crowd the interval $[sE_0, sE_1]$, and the variational approach no longer applies. Instead, a resolvent identity combined with the Sherman-Morrison formula for rank-one perturbations tracks the gap through this congested region. The resulting piecewise linear profile — steep on the left, shallower on the right, flat in the window — feeds directly into the runtime calculation of Chapter 7.

## 6.1 Gap to the Left of the Crossing

The eigenvalue equation (Lemma 5.3.1) places the ground state energy at $\lambda_0(s) < sE_0$ and the first excited energy at $\lambda_1(s) \in (sE_0, sE_1)$. The gap $g(s) = \lambda_1(s) - \lambda_0(s)$ is therefore positive, but these bounds alone give only the trivial estimate $g(s) < s\Delta$. For the runtime integral, we need a tight lower bound that captures the linear growth of the gap as $s$ decreases away from $s^*$.

The strategy is to tighten the upper bound on $\lambda_0(s)$. Two approaches give the same result. The first uses the variational principle: for any normalized state $|\phi\rangle$, the ground energy satisfies $\lambda_0(s) \le \langle\phi|\, H(s)\, |\phi\rangle$, so a well-chosen ansatz produces a quantitative upper bound. The second uses concavity: since $\lambda_0(s) = \min_{|\psi\rangle} \langle\psi|\, H(s)\, |\psi\rangle$ is the pointwise minimum of affine functions in $s$, it is concave, and any tangent line lies above it. The variational approach is more direct — it produces the bound in a single calculation — so we present it here.

**Lemma 6.1.1** (Gap to the left of the crossing)**.** *For any $s \in \mathcal{I}_{s\leftarrow} = [0,\, s^* - \delta_s)$, the spectral gap of $H(s)$ satisfies*

$$g(s) \ge \frac{A_1(A_1+1)}{A_2}\,(s^* - s)\,. \tag{6.1.1}$$

*Proof.* We upper-bound $\lambda_0(s)$ via the variational principle and lower-bound $\lambda_1(s)$ from the eigenvalue equation.

The ansatz must live in the span of $\{|k\rangle : k \ge 1\}$, orthogonal to the ground-state component $|0\rangle$, and should concentrate amplitude on levels close to $E_0$ where the energy expectation is lowest. The natural weighting is the inverse energy gap: levels near $E_0$ receive more amplitude. Requiring unit norm fixes the overall scale, giving

$$|\phi\rangle = \frac{1}{\sqrt{A_2 N}} \sum_{k=1}^{M-1} \frac{\sqrt{d_k}}{E_k - E_0}\, |k\rangle\,. \tag{6.1.2}$$

This weighting arises naturally in first-order perturbation theory: the correction to the ground state of $sH_z$ due to the perturbation $-(1-s)\,|\psi_0\rangle\langle\psi_0|$ has exactly this form. Normalization is immediate:

$$\langle\phi\rangle\,\phi = \frac{1}{A_2 N} \sum_{k=1}^{M-1} \frac{d_k}{(E_k - E_0)^2} = \frac{A_2}{A_2} = 1. \tag{6.1.3}$$

To compute $\langle\phi| H(s) |\phi\rangle$, decompose $H(s) = -(1-s)|\psi_0\rangle\langle\psi_0| + s(H_z - E_0) + sE_0$. Each term contributes separately.

The projector term gives

$$-(1-s)\left|\langle\psi_0|\phi\rangle\right|^2 = -(1-s)\left(\frac{1}{\sqrt{A_2 N}}\sum_{k=1}^{M-1}\frac{d_k}{(E_k-E_0)\sqrt{N}}\right)^2 = -(1-s)\frac{A_1^2}{A_2}, \tag{6.1.4}$$

where $\langle\psi_0|\phi = A_1/\sqrt{A_2}$ follows from $\langle\psi_0|k\rangle = \sqrt{d_k/N}$ and the definition of $A_1$.

The shifted diagonal term gives

$$s\langle\phi|(H_z - E_0)|\phi\rangle = \frac{s}{A_2 N}\sum_{k=1}^{M-1}\frac{d_k}{(E_k-E_0)^2}\cdot(E_k-E_0) = \frac{s}{A_2 N}\sum_{k=1}^{M-1}\frac{d_k}{E_k-E_0} = \frac{s\,A_1}{A_2}. \tag{6.1.5}$$

The constant term contributes $sE_0\langle\phi|\phi = sE_0$. Combining:

$$\lambda_0(s) \le \langle\phi|H(s)|\phi\rangle = sE_0 - (1-s)\frac{A_1^2}{A_2} + s\frac{A_1}{A_2} = sE_0 + \frac{A_1}{A_2}\left(s(1+A_1) - A_1\right). \tag{6.1.6}$$

Since $s^*(1+A_1) = A_1$, we have $s(1+A_1) - A_1 = (1+A_1)(s-s^*) = (s-s^*)/(1-s^*)$, so

$$\lambda_0(s) \le sE_0 + \frac{A_1}{A_2}\cdot\frac{s-s^*}{1-s^*}. \tag{6.1.7}$$

For $s < s^*$, the second term is negative, confirming $\lambda_0(s) < sE_0$.

For the first excited state, the eigenvalue equation (Lemma 5.3.1) confines $\lambda_1(s)$ to the interval $(sE_0, sE_1)$, so

$$\lambda_1(s) \ge sE_0. \tag{6.1.8}$$

The gap is therefore

$$g(s) = \lambda_1(s) - \lambda_0(s) \ge sE_0 - sE_0 - \frac{A_1}{A_2}\cdot\frac{s-s^*}{1-s^*} = \frac{A_1}{A_2}\cdot\frac{s^*-s}{1-s^*}. \tag{6.1.9}$$

Since $1/(1-s^*) = A_1 + 1$, we obtain $g(s) \ge A_1(A_1+1)(s^*-s)/A_2$. □

At the left boundary of the crossing window, $s = s^* - \delta_s$, the bound gives

$$g(s^*-\delta_s) \ge \frac{A_1(A_1+1)}{A_2}\cdot\delta_s = \hat{g} \ge \frac{g_{\min}}{1-2\eta}, \tag{6.1.10}$$

using $A_1(A_1+1)\delta_s/A_2 = \hat{g}$ from Eq. (5.4.10) (equivalently, $A_1 = s^*(A_1+1)$) and $g_{\min} \ge (1-2\eta)\hat{g}$ from Eq. (5.4.9). The gap at the window boundary exceeds $g_{\min}$, confirming that the minimum gap lies within $\mathcal{I}_{s^*}$.

The same bound follows from concavity. The second derivative of $\lambda_0(s)$ satisfies

$$\ddot{\lambda}_0(s) = -2\sum_{j\ge1}|\langle\phi_j(s)|\dot{H}|\phi_0(s)\rangle|^2/(E_j(s)-E_0(s)) \le 0$$

where $\dot{H} = H_z + |\psi_0\rangle\langle\psi_0|$ and $|\phi_j(s)\rangle$ are the instantaneous eigenstates. The tangent to the concave function $\lambda_0(s)$ at $s = s^*$ lies above it everywhere, and its slope evaluated using Eq. (6.1.7) reproduces the same linear bound.

For the running example ($M = 2$, $d_0 = 1$, $d_1 = N-1$, $E_0 = 0$, $E_1 = 1$), the ansatz reduces to $|\phi\rangle = |1\rangle$, and the bound becomes

$$g(s) \ge \frac{(N-1)/N\cdot(2N-1)/N}{(N-1)/N}\left(\frac{1}{2}-s\right) = \frac{2N-1}{N}\left(\frac{1}{2}-s\right) \approx 2\left(\frac{1}{2}-s\right). \tag{6.1.11}$$

The exact gap $g(s) = \sqrt{(2s-1)^2 + 4s(1-s)/N}$ at $s = 1/4$ equals $\sqrt{1/4 + 3/(4N)} \approx 1/2$, while the bound gives $(2N-1)/(4N) \approx 1/2$. The bound is tight near $s^*$ and only becomes loose as $s$ approaches 0, where the true gap approaches 1 while the bound continues growing. Since the runtime integral is dominated by the crossing window, this looseness far from $s^*$ has negligible effect.

## 6.2 Gap to the Right of the Crossing

Bounding the spectral gap to the right of $s^*$ is the main technical challenge of this chapter. The variational principle that worked on the left does not extend: it provides upper bounds on $\lambda_0(s)$, but what we need on the right is a lower bound on $\lambda_1(s) - \lambda_0(s)$ that captures the linear reopening of the gap. The variational principle bounds ground energies from above, not excited energies from below.

The obstacle is structural. On the left, the first excited eigenvalue $\lambda_1(s)$ is bounded below by $sE_0$ from the eigenvalue equation, giving a clean reference point. On the right, $\lambda_1(s)$ lies between $sE_0$ and $sE_1$, but so do eigenvalues from the higher levels of $sH_z$, which undergo their own avoided crossings with the first excited state. Tracking $\lambda_1(s)$ through this congested region requires a tool that bounds the distance from a given point to the spectrum without identifying individual eigenvalues.

The resolvent provides exactly this. For a self-adjoint operator $A$ with spectrum $\sigma(A)$ and any $\lambda \notin \sigma(A)$, the resolvent

$$R_A(\lambda) = (\lambda I - A)^{-1} \tag{6.2.1}$$

is a bounded operator whose norm equals the inverse distance from $\lambda$ to the spectrum:

$$\|R_A(\lambda)\| = \frac{1}{\operatorname{dist}(\lambda,\, \sigma(A))}. \tag{6.2.2}$$

This follows from the spectral theorem: in the eigenbasis of $A$ with eigenvalues $\{\lambda_j\}$, the resolvent is diagonal with entries $1/(\lambda - \lambda_j)$, and its operator norm is the maximum absolute value $\max_j |1/(\lambda - \lambda_j)| = 1/\min_j |\lambda - \lambda_j|$. If a point $\gamma$ lies between two consecutive eigenvalues $\lambda_0$ and $\lambda_1$, then $\operatorname{dist}(\gamma, \sigma(A)) = \min(\gamma - \lambda_0, \lambda_1 - \gamma) \leq g/2$, since the minimum of two non-negative numbers summing to $g$ is at most $g/2$. Therefore $\|R_A(\gamma)\| = 1/\operatorname{dist}(\gamma, \sigma(A)) \geq 2/g$, and the useful contrapositive is

$$g(s) \geq \frac{2}{\|R_{H(s)}(\gamma)\|}. \tag{6.2.3}$$

Bounding the gap from below reduces to bounding the resolvent norm from above.

The adiabatic Hamiltonian $H(s) = sH_z - (1-s)\,|\psi_0\rangle\langle\psi_0|$ is a rank-one perturbation of $sH_z$. Rank-one perturbations have a classical inversion formula. The Sherman-Morrison identity [13] states that for an invertible operator $A$ and vectors $|u\rangle, \langle v|$,

$$(A + |u\rangle\langle v|)^{-1} = A^{-1} - \frac{A^{-1}\,|u\rangle\langle v|\,A^{-1}}{1 + \langle v|\,A^{-1}\,|u\rangle}, \tag{6.2.4}$$

provided $1 + \langle v|\,A^{-1}\,|u\rangle \neq 0$. Applying this to the resolvent of $H(s)$ decomposes it into the resolvent of $sH_z$ (whose spectrum is known explicitly) and a correction from the rank-one term $-(1-s)\,|\psi_0\rangle\langle\psi_0|$. The triangle inequality then yields an upper bound on $\|R_{H(s)}(\gamma)\|$.

The strategy is: choose a line $\gamma(s)$ that lies between $\lambda_0(s)$ and $\lambda_1(s)$ for all $s \geq s^*$, apply the Sherman-Morrison decomposition, bound each piece using the spectral parameters $A_1$ and $A_2$, and show that the resulting bound on $\|R_{H(s)}(\gamma)\|$ yields a linear lower bound on $g(s)$.

The simplest choice for $\gamma(s)$ is a line starting at $sE_0$ when $s = s^*$ and ending between $E_0$ and $E_1$ at $s = 1$: take $\beta(s) = a(s - s^*)/(1 - s^*)$ with $a < \Delta$ and set $\gamma(s) = sE_0 + \beta(s)$. With $a = \Delta/6$, the function $f(s)$ controlling the resolvent bound can be shown to satisfy $f(s) \leq 1$ for all $s \geq s^*$, giving $g(s) \geq \beta(s) = (\Delta/6)(s - s^*)/(1 - s^*)$. This bound has a problem: at the window boundary $s = s^* + \delta_s$, it gives $g(s^* + \delta_s) \geq (\Delta/6) \cdot \delta_s/(1 - s^*) = (\Delta A_2)/(3A_1) \cdot g_{\min}$. Since $\Delta A_2 \leq A_1$, this is at most $g_{\min}/3$, and for Hamiltonians with $\Delta A_2 \ll A_1$, it can be polynomially smaller than $g_{\min}$. At $s = s^*$ itself, the bound gives $g(s^*) \geq 0$, missing the true gap entirely.

The failure has a geometric explanation. At $s^*$, the ground energy $\lambda_0(s^*)$ is not at $s^*E_0$ but rather $g_{\min}/2$ below it. The line $\gamma(s)$ passes through $s^*E_0$ at $s = s^*$, so it sits between the two eigenvalues but with zero margin below. The resolvent norm at a point equidistant from two eigenvalues has norm $2/g$, but at a point touching one eigenvalue, the norm diverges. The line must start with $O(g_{\min})$ separation from both eigenvalues at $s^*$.

The fix is to shift the line's origin from $s^*$ to a point $s_0 < s^*$ so that $\beta(s^*) = k\, g_{\min}$ for a constant $k < 1$. With $\beta(s) = a(s - s_0)/(1 - s_0)$, the constraint $\beta(s^*) = k\, g_{\min}$ determines

$$s_0 = s^* - \frac{k\, g_{\min}(1 - s^*)}{a - k\, g_{\min}}. \tag{6.2.5}$$

The line now passes through $\gamma(s^*) = s^*E_0 + k\, g_{\min}$, which lies between $\lambda_0(s^*)$ and $\lambda_1(s^*)$ when $k$ is chosen appropriately. The price is that $s_0 < s^*$ introduces additional terms in the monotonicity analysis for $f(s)$, requiring a careful choice of $a$.

**Lemma 6.2.1** (Gap to the right of the crossing). *Let $k = 1/4$, $a = 4k^2\Delta/3 = \Delta/12$, and $s_0$ as in Eq. (6.2.5). Then for all $s \geq s^*$, the spectral gap of $H(s)$ satisfies*

$$g(s) \geq \frac{\Delta}{30} \cdot \frac{s - s_0}{1 - s_0}. \tag{6.2.6}$$

*Proof.* Set $\gamma(s) = sE_0 + \beta(s)$ with $\beta(s) = a(s - s_0)/(1 - s_0)$. We bound $\|R_{H(s)}(\gamma)\|$ from above using the Sherman-Morrison formula.

Since $H(s) = sH_z - (1 - s)\,|\psi_0\rangle\langle\psi_0|$, the resolvent of $H(s)$ at $\gamma$ satisfies, via Eq. (6.2.4) and the triangle inequality,

$$\|R_{H(s)}(\gamma)\| \leq \|R_{sH_z}(\gamma)\| + (1 - s)\frac{\|R_{sH_z}(\gamma)\,|\psi_0\rangle\langle\psi_0|\,R_{sH_z}(\gamma)\|}{1 + (1 - s)\,\langle\psi_0|\,R_{sH_z}(\gamma)\,|\psi_0\rangle}. \tag{6.2.7}$$

The unperturbed resolvent $R_{sH_z}(\gamma)$ is diagonal in the $|k\rangle$ basis with entries $1/(\gamma - sE_k) = 1/(\beta - s(E_k - E_0))$ for $k \geq 1$ and $1/\beta$ for $k = 0$. The nearest eigenvalue of $sH_z$ to $\gamma$ is $sE_0$, at distance $\beta$, so $\|R_{sH_z}(\gamma)\| = 1/\beta$.

We bound the numerator and denominator of the second term separately. Both require that $\beta(s) \leq s(E_k - E_0)/2$ for all $k \geq 1$, which ensures the Taylor expansion in powers of $\beta/(s(E_k - E_0))$ converges rapidly. Since $\beta(s) \leq a = \Delta/12$ and $s(E_k - E_0) \geq s^*\Delta \geq \Delta/3$ (using $s^* = A_1/(A_1 + 1) \geq 1/3$, which holds when $A_1 \geq 1/2$, i.e., $d_0 \leq N/2$), we have $\beta \leq \Delta/12 < \Delta/6 \leq s(E_k - E_0)/2$. When $d_0 > N/2$, the majority of states are ground states and random sampling finds a solution with constant probability, making the adiabatic approach unnecessary.

**Numerator bound.** The squared norm of $R_{sH_z}(\gamma)\,|\psi_0\rangle$ expands as

$$\|R_{sH_z}(\gamma)\,|\psi_0\rangle\|^2 = \frac{d_0}{N\beta^2} + \frac{1}{N}\sum_{k=1}^{M-1}\frac{d_k}{(s(E_k - E_0) - \beta)^2}. \tag{6.2.8}$$

Using $s(E_k - E_0) - \beta \geq s(E_k - E_0)/2$, each term in the sum is at most $4d_k/(Ns^2(E_k - E_0)^2)$, giving

$$\|R_{sH_z}(\gamma)\,|\psi_0\rangle\langle\psi_0|\,R_{sH_z}(\gamma)\| \leq \|R_{sH_z}(\gamma)\,|\psi_0\rangle\|^2 \leq \frac{d_0}{N\beta^2} + \frac{4A_2}{s^2}. \tag{6.2.9}$$

**Denominator bound.** Expanding the expectation value:

$$\begin{aligned} 1 + (1 - s)\,\langle\psi_0|\,R_{sH_z}(\gamma)\,|\psi_0\rangle &= 1 + \frac{(1 - s)d_0}{N\beta} - \frac{1 - s}{N}\sum_{k=1}^{M-1}\frac{d_k}{s(E_k - E_0) - \beta} \\ &= 1 + \frac{(1 - s)d_0}{N\beta} - \frac{1 - s}{s}\sum_{k=1}^{M-1}\frac{d_k}{N(E_k - E_0)}\sum_{\ell=0}^{\infty}\left(\frac{\beta}{s(E_k - E_0)}\right)^{\ell}. \end{aligned} \tag{6.2.10}$$

Using $\beta/(s(E_k - E_0)) \leq 1/2$ to bound the geometric series by $1 + 2\beta/(s(E_k - E_0))$:

$$1 + (1 - s)\,\langle\psi_0|\,R_{sH_z}(\gamma)\,|\psi_0\rangle \geq 1 + \frac{(1 - s)d_0}{N\beta} - (1 - s)\left(\frac{A_1}{s} + \frac{2A_2\beta}{s^2}\right). \tag{6.2.11}$$

**Collecting terms.** Substituting the bounds (6.2.9) and (6.2.11) into (6.2.7) and factoring:

$$\|R_{H(s)}(\gamma)\| \leq \frac{1}{\beta}\,(1 + f(s))\,, \tag{6.2.12}$$

where, writing $\epsilon_0 = d_0/N$,

$$f(s) = \frac{\epsilon_0\, s^2(1 - s) + 4A_2\beta^2(1 - s)}{\epsilon_0\, s^2(1 - s) + \beta\, s\,\dfrac{s - s^*}{1 - s^*} - 2A_2\beta^2(1 - s)}. \tag{6.2.13}$$

To obtain this form, multiply numerator and denominator of the second term in (6.2.7) by $\beta$, then multiply by $s^2(1 - s)$ to clear fractions. The key step is rewriting the denominator's constant-plus-linear terms. Using $A_1 = s^*/(1 - s^*)$:

$$1 - \frac{(1 - s)A_1}{s} + \frac{(1 - s)\epsilon_0}{\beta} = \frac{s - s^*}{s(1 - s^*)} + \frac{(1 - s)\epsilon_0}{\beta}, \tag{6.2.14}$$

since $1 - A_1(1 - s)/s = (s - A_1(1 - s))/s = (s - s^*(1 - s)/(1 - s^*))/s = (s(1 - s^*) - s^*(1 - s))/(s(1 - s^*)) = (s - s^*)/(s(1 - s^*))$. Multiplying through by $\beta s^2(1 - s)$ and collecting the Taylor-bounded terms into the $A_2\beta^2$ contributions gives Eq. (6.2.13).

The numerator of $f(s)$ measures the rank-one perturbation's effect on the resolvent: the $\epsilon_0$ term comes from the $|0\rangle$ component of $|\psi_0\rangle$ (the ground-state overlap), while the $A_2$ term comes from the excited components. The denominator captures the spectral rigidity: the term $\beta\, s(s-s^*)/(1-s^*)$ grows as $\gamma$ moves away from the crossing, stabilizing the resolvent against the perturbation. Near $s^*$, the denominator is small (the gap is small), so $f(s^*)$ is $O(1)$. As $s$ increases, the denominator grows and $f(s) \to 0$.

From (6.2.12) and (6.2.3), the spectral gap satisfies

$$g(s) \geq \frac{2\beta(s)}{1+f(s)} \geq \frac{2\beta(s)}{1+\max_{s\geq s^*} f(s)}. \tag{6.2.15}$$

If $f$ is monotonically decreasing on $[s^*, 1]$, then $\max_{s\geq s^*} f(s) = f(s^*)$, and the bound becomes $g(s) \geq 2\beta(s)/(1+f(s^*))$, which is linear in $s - s_0$.

**Monotonicity of $f$.** We show $f'(s) < 0$ for $s \in [s^*, 1]$. Write $f = u/v$ with

$$\begin{aligned} u &= \epsilon_0\, s^2(1-s) + 4A_2\beta^2(1-s), \\ v &= \epsilon_0\, s^2(1-s) + \beta\, s\,\frac{s-s^*}{1-s^*} - 2A_2\beta^2(1-s). \end{aligned} \tag{6.2.16}$$

Then $f' = (u'v - uv')/v^2$, so the sign of $f'$ is determined by $u'v - uv'$.

Computing $u'$ and $v'$ using $\beta' = a/(1-s_0)$:

$$\begin{aligned} u' &= \frac{4aA_2\beta}{1-s_0}(2+s_0-3s) + \epsilon_0\, s(2-3s), \\ v' &= \frac{a(3s^2 - 2s(s^*+s_0) + s^*s_0)}{(1-s_0)(1-s^*)} - \frac{2aA_2\beta}{1-s_0}(2+s_0-3s) + \epsilon_0\, s(2-3s). \end{aligned} \tag{6.2.17}$$

Expanding $u'v$ and $uv'$ and taking the difference, two terms cancel exactly: the $\epsilon_0^2 s^3(2-3s)(1-s)$ term and the $8aA_2^2\beta^3(1-s)(2+s_0-3s)/(1-s_0)$ term. The remaining expression has three terms [10]:

$$\begin{aligned} u'v - uv' = &-\frac{4aA_2\beta^2}{(1-s_0)(1-s^*)}\Big(s^2(1+s_0-s^*) - 2s\,s_0 + s^*s_0\Big) \\ &+ \frac{12aA_2\epsilon_0\,\beta}{1-s_0}\, s(1-s)^2\, s_0 \\ &- \frac{\epsilon_0\, s^2 a}{(1-s_0)(1-s^*)}\Big(-s^2(s^*+s_0-1) + 2s\,s_0 s^* - s^*s_0\Big). \end{aligned} \tag{6.2.18}$$

The first and third terms are negative; the second is positive (it is the only term involving $\epsilon_0\, s_0$, which arises from the shift of $s_0$ below $s^*$). We must show the first negative term dominates the positive one.

Factor out $-4aA_2\beta/(1-s_0)$ from the sum of the first two terms:

$$-\frac{4aA_2\beta}{1-s_0}\left(\frac{\beta}{1-s^*}\Big(s^2(1+s_0-s^*) - 2s\,s_0 + s^*s_0\Big) - 3\epsilon_0\, s_0\, s(1-s)^2\right). \tag{6.2.19}$$

The quadratic $s^2(1+s_0-s^*) - 2s\,s_0 + s^*s_0$ is a convex function of $s$ that is minimized at some $s_m < s^*$ and is positive for $s \geq s^*$. The cubic $s(1-s)^2$ is maximized at $s = 1/3 \leq s^*$. Therefore, on $[s^*, 1]$, the bracket in (6.2.19) is bounded below by its value at $s = s^*$:

$$\frac{a(s^*-s_0)^2}{1-s_0} - 3\epsilon_0\, s_0(1-s^*)^2. \tag{6.2.20}$$

Using $s_0 \leq s^*$ and $s^* - s_0 = k\, g_{\min}(1-s^*)/(a - k\, g_{\min})$, this is positive whenever

$$a < \frac{4}{3}k^2\frac{A_1}{A_2}. \tag{6.2.21}$$

Since $\Delta A_2 \leq A_1$ (because $A_2 \leq \sum_{k\geq 1} d_k/(N(E_k-E_0)^2) \leq A_1/\Delta$), the choice $a = (4/3)k^2\Delta$ satisfies (6.2.21). With this choice, $u'v - uv' < 0$ on $[s^*, 1]$, so $f$ is monotonically decreasing.

**Evaluating $f(s^*)$.** At $s = s^*$, $\beta(s^*) = k\, g_{\min}$. The term $\beta\, s(s-s^*)/(1-s^*)$ vanishes, so

$$f(s^*) = \frac{\epsilon_0\, {s^*}^2(1-s^*) + 4A_2k^2g_{\min}^2(1-s^*)}{\epsilon_0\, {s^*}^2(1-s^*) - 2A_2k^2g_{\min}^2(1-s^*)}. \tag{6.2.22}$$

Using $g_{\min} \approx (2s^*/\sqrt{A_2})\sqrt{\epsilon_0}$ (from Eq. (5.4.9) with $\hat{g} = 2s^*\sqrt{\epsilon_0/A_2}$), we have $A_2 k^2 g_{\min}^2 \approx 4k^2 s^{*2}\epsilon_0$. Substituting:

$$f(s^*) = \frac{1+16k^2}{1-8k^2}. \tag{6.2.23}$$

For $k = 1/4$: $f(s^*) = (1+1)/(1-1/2) = 4$, so $1 + f(s^*) = 5$.

**Final bound.** From (6.2.15):

$$g(s) \geq \frac{2\beta(s)}{1+f(s^*)} = \frac{2a}{1+f(s^*)} \cdot \frac{s-s_0}{1-s_0}. \tag{6.2.24}$$

The prefactor evaluates to

$$\frac{2a}{1+f(s^*)} = \frac{2\cdot(4/3)k^2\Delta}{1+(1+16k^2)/(1-8k^2)} = \frac{4}{3}k^2 \cdot \frac{1-8k^2}{1+4k^2} \cdot \Delta. \tag{6.2.25}$$

The function $P(k) = (4/3)k^2(1-8k^2)/(1+4k^2)$ is maximized at $k_{\text{opt}} = \frac{1}{2}\sqrt{\sqrt{3/2}-1} \approx 0.237$, where $P(k_{\text{opt}}) = \frac{1}{3}(5-2\sqrt{6}) \approx 0.034$. For $k = 1/4$:

$$P(1/4) = \frac{4}{3}\cdot\frac{1}{16}\cdot\frac{1/2}{5/4} = \frac{1}{30}. \tag{6.2.26}$$

Therefore $g(s) \geq (\Delta/30)(s-s_0)/(1-s_0)$. □

For the running example ($M = 2$, $\Delta = 1$), the bound gives $g(s) \geq (1/30)(s-s_0)/(1-s_0)$, where $s_0 = 1/2 - O(1/\sqrt{N})$ is close to $s^* \approx 1/2$ for large $N$. Near $s = 3/4$, the exact gap from Eq. (5.3.15) is $g(3/4) = \sqrt{1/4 + 3/(16N)} \approx 1/2$, while the bound gives approximately $(1/30)(1/4)/(1/2) = 1/60$. The bound is conservative by a factor of approximately 30 but correctly captures the linear growth. This constant is the price of a clean, uniform bound valid for all problem Hamiltonians satisfying the spectral condition.

## 6.3 The Complete Gap Profile

Combining the results of this chapter with those of Chapter 5, the spectral gap $g(s)$ is bounded below across all of $[0,1]$.

**Theorem 6.3.1** (Complete gap profile)**.** *Let $H_z$ satisfy the spectral condition (Definition 5.2.2). The spectral gap of $H(s) = -(1-s)\,|\psi_0\rangle\langle\psi_0| + sH_z$ satisfies, for all $s \in [0,1]$:*

$$g(s) \geq \begin{cases} \dfrac{A_1(A_1+1)}{A_2}\,(s^*-s)\,, & s \in \mathcal{I}_{s\leftarrow} = [0,\, s^*-\delta_s)\,, \\ g_{\min}, & s \in \mathcal{I}_{s^*} = [s^*-\delta_s,\, s^*+\delta_s]\,, \\ \dfrac{\Delta}{30}\cdot\dfrac{s-s_0}{1-s_0}, & s \in \mathcal{I}_{s\rightarrow} = (s^*+\delta_s,\, 1]\,, \end{cases} \tag{6.3.1}$$

*where $s_0 = s^* - k\,g_{\min}(1-s^*)/(a - k\,g_{\min})$ with $k = 1/4$ and $a = \Delta/12$.*

*Proof.* The three cases follow from Lemma 5.4.2 (window, proved in Chapter 5), Lemma 6.1.1 (left), and Lemma 6.2.1 (right). The right bound holds for all $s \geq s^*$ and therefore covers $\mathcal{I}_{s\rightarrow}$. The window bound $g(s) \geq g_{\min}$ is tighter than the right bound at $s^*$ but weaker far from the crossing. □

The bounds match across region boundaries. At the left boundary $s = s^* - \delta_s$:

$$\frac{A_1(A_1+1)}{A_2}\cdot\delta_s = \hat{g} \geq \frac{g_{\min}}{1-2\eta} > g_{\min}, \tag{6.3.2}$$

so the left bound exceeds the window bound. At $s = s^*$, the right bound gives $g(s^*) \geq 2\beta(s^*)/(1+f(s^*)) = 2k\,g_{\min}/5 = g_{\min}/10$, which is below $g_{\min}$ by a constant factor but still $O(g_{\min})$. The window bound provides the tighter estimate $g(s^*) = g_{\min}$.

The gap profile has a characteristic shape. It forms a broad V centered at $s^*$, with a narrow rounded minimum of width approximately $2\delta_s$. The left arm has slope $A_1(A_1+1)/A_2$, which is $O(\text{poly}(n))$ for Ising Hamiltonians. The right arm has the shallower slope $\Delta/(30(1-s_0))$, controlled by the spectral gap $\Delta$ of the

problem Hamiltonian. The asymmetry in the bounds — steep on the left, shallow on the right — is a proof artifact: the variational bound captures the true slope closely, while the resolvent bound sacrifices tightness for uniform validity across a more complicated spectral landscape. At the endpoints, $g(0) = 1$ (the initial gap between eigenvalues $-1$ and 0 of $H_0$) and $g(1) = \Delta$ (the gap of $H_z$).

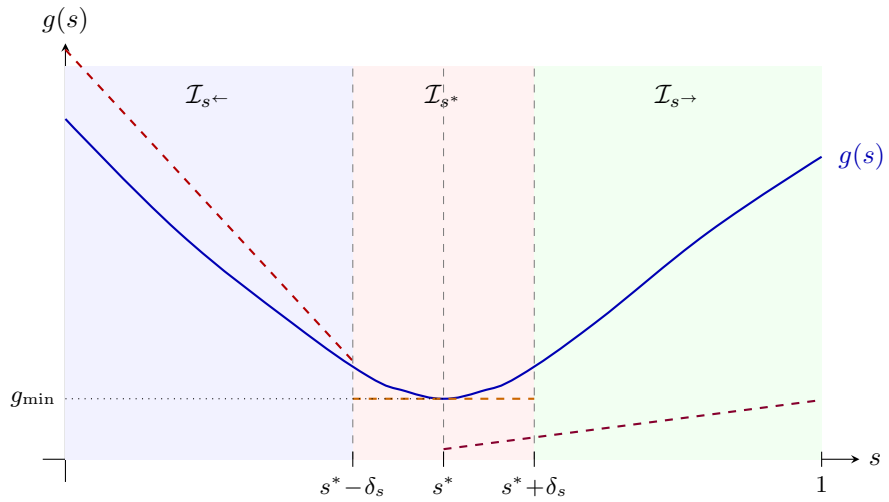


Figure 6.1: Schematic gap profile for $H(s)$. The solid curve shows the true spectral gap $g(s)$, which dips to $g_{\min}$ at $s = s^*$ and rises on both sides. The dashed lines show the piecewise lower bounds: linear on the left (steep), constant in the window, and linear on the right (shallower). The three regions $\mathcal{I}_{s\leftarrow}$, $\mathcal{I}_{s^*}$, $\mathcal{I}_{s\rightarrow}$ are indicated.

Given any problem Hamiltonian $H_z$ satisfying the spectral condition, the gap is bounded across $[0, 1]$ by the piecewise profile of Theorem 6.3.1, determined up to constant factors by $A_1$, $A_2$, $d_0$, and $\Delta$. The minimum gap $g_{\min} = \Theta(\sqrt{d_0/(NA_2)})$ occurs at $s^* = A_1/(A_1 + 1)$ and is exponentially small in $n$ when $d_0 = O(1)$. The crossing position depends only on $A_1$, not on $A_2$ or $d_0$. More solutions (larger $d_0$) widen the gap; richer spectral structure (larger $A_2$) narrows it. The gap reaches $\Delta$ at $s = 1$, the spectral gap of the problem Hamiltonian itself.

For the running example, the exact gap $g(s) = \sqrt{(2s-1)^2 + 4s(1-s)/N}$ and the piecewise bound from Theorem 6.3.1 can be compared directly. The left bound has slope approximately 2, matching the exact slope $|g'(s^*)| = 2\sqrt{1 - 1/N} \approx 2$. The window bound $g_{\min} = 1/\sqrt{N}$ is exact. The right bound has slope approximately $1/15$ near $s^*$, weaker than the true slope by a factor of 30, but sufficient for the runtime integral since the window dominates.

The runtime integral $\int_0^1 g(s)^{-2}\, ds$ splits across the three regions. In the left and right regions, $g(s) \sim C|s - s^*|$ for constants $C$, and

$$\int_{\delta_s}^{s^*} \frac{du}{(Cu)^2} = \frac{1}{C^2}\left(\frac{1}{\delta_s} - \frac{1}{s^*}\right) \leq \frac{1}{C^2\delta_s}, \tag{6.3.3}$$

which is $O(1/(C^2\delta_s))$. In the window, $g(s) \geq g_{\min}$ gives $\int_{s^*-\delta_s}^{s^*+\delta_s} g(s)^{-2}\, ds \leq 2\delta_s/g_{\min}^2$. The window contribution $\delta_s/g_{\min}^2 = \Theta(A_2^{3/2}/A_1^2 \cdot \sqrt{N/d_0})$ dominates the outer regions, and the full integral — including the $\Delta$-dependent right-arm contribution — yields the runtime $T = O((\sqrt{A_2}/(A_1^2\Delta^2))\sqrt{N/d_0})$ that Chapter 7 derives rigorously.

# Chapter 7

# Optimal Schedule

The spectral gap of $H(s)$ is now bounded below across all of $[0,1]$: a piecewise linear profile (Theorem 6.3.1) that dips to $g_{\min}$ at the avoided crossing $s^*$ and rises linearly on both sides, with slope $A_1(A_1+1)/A_2$ on the left and $\Delta/30$ on the right. Chapter 5 observed that the runtime scales as $\int_0^1 g(s)^{-2}\,ds$ (Eq. (5.5.6)), with the crossing window dominating. This chapter derives the optimal schedule and the resulting runtime rigorously.

The standard adiabatic theorem, applied with a constant evolution rate, gives a runtime proportional to $\int_0^1 g(s)^{-3}\,ds$. For the gap profile of Theorem 6.3.1, the window contributes $\delta_s/g_{\min}^3$, which for the running example ($M=2$, $g_{\min}=1/\sqrt{N}$) gives $T=O(N)$: no speedup over classical search. The remedy is a local adaptive schedule whose rate $K'(s)$ scales with the instantaneous gap, evolving rapidly where the gap is large and slowly near the crossing. This idea, originating with Roland and Cerf [1] for the single-marked-item case and developed in the eigenpath traversal framework [14, 15], extends to general problem Hamiltonians through the adiabatic error bound of [10]. The resulting runtime is $T=O((\sqrt{A_2}/(A_1(A_1+1)\Delta^2))\sqrt{N/d_0}/\varepsilon)$, achieving the Grover speedup up to spectral factors.

## 7.1 The Adiabatic Error Bound

The Schrödinger equation $i\,d\,|\psi\rangle/dt = H(s(t))\,|\psi\rangle$ governs the evolution of a quantum state under the time-dependent Hamiltonian $H(s)$, where $s:[0,T]\to[0,1]$ parametrizes the interpolation and $T$ is the total evolution time. The density matrix formulation $d\rho/dt=-i[H,\rho]$ accommodates mixed states and simplifies the error analysis. Introduce a reparametrization $t=K(s)$, where $K:[0,1]\to\mathbb{R}^+$ is a differentiable, monotonically increasing function called the *schedule*. The chain rule transforms the evolution equation to

$$\frac{d\rho}{ds} = -iK'(s)[H(s),\rho(s)], \tag{7.1.1}$$

where $K'(s)=dK/ds>0$ controls the instantaneous evolution rate. The total runtime is $T=K(1)=\int_0^1 K'(s)\,ds$. A large $K'(s)$ means slow evolution (long physical time per unit of $s$), allowing the state to track the ground state through a small-gap region. A small $K'(s)$ means fast evolution, appropriate where the gap is large and diabatic transitions are suppressed.

The error of the adiabatic evolution is the probability that the final state does not lie in the ground space of $H(1)$:

$$\varepsilon = 1-\mathrm{Tr}[P(1)\rho(1)], \tag{7.1.2}$$

where $P(s)$ denotes the projector onto the ground eigenspace of $H(s)$ and $\rho(0)=P(0)$ (the system starts in the ground state of $H(0)$). The projector $P(s)$ and the ground energy $\lambda_0(s)$ are both functions of $s$, varying as the Hamiltonian interpolates from $H_0$ to $H_z$. The operator

$$(H(s)-\lambda_0(s))^+ = \sum_{j\geq 1}\frac{1}{\lambda_j(s)-\lambda_0(s)}\,|\phi_j(s)\rangle\langle\phi_j(s)| \tag{7.1.3}$$

is the pseudoinverse of $H(s)-\lambda_0(s)$: it acts as zero on the ground space and as $(\lambda_j-\lambda_0)^{-1}$ on the $j$-th excited eigenspace. Its operator norm is $1/g(s)$, so a small spectral gap amplifies the pseudoinverse.

**Lemma 7.1.1** (Adiabatic error bound [10, 15])**.** *Let $H(s)$ be a twice-differentiable path of Hamiltonians with a continuous ground energy $\lambda_0(s)$ and a spectral gap $g(s)>0$ for all $s\in[0,1]$. Let $K:[0,1]\to\mathbb{R}^+$ be a schedule*

*with absolutely continuous derivative $K'$. Then the evolution (7.1.1) starting from $\rho(0) = P(0)$ satisfies*

$$\varepsilon \le \frac{1}{K'(1)} \left\| \left[P'(1),\, (H(1) - \lambda_0(1))^+\right] \right\| + \int_0^1 \frac{1}{K'} \left\| \left[P',\, (H - \lambda_0)^+\right]' \right\| ds + \int_0^1 \left| \left(\frac{1}{K'}\right)' \right| \left\| \left[P',\, (H - \lambda_0)^+\right] \right\| ds. \tag{7.1.4}$$

The proof proceeds by tracking the fidelity $\mathrm{Tr}[P(s)\rho(s)]$ as a function of $s$. Differentiating and using $HP = \lambda_0 P$ yields $d(\mathrm{Tr}[P\rho])/ds = i(K')^{-1}\mathrm{Tr}([P', (H-\lambda_0)^+]\rho')$. Integrating by parts transfers derivatives from $\rho$ onto the commutator $[P', (H-\lambda_0)^+]$ and the schedule factor $(K')^{-1}$, producing three terms. The boundary term at $s = 0$ vanishes because $\rho(0) = P(0)$ lies entirely in the ground space, and the commutator $[P', (H-\lambda_0)^+]$ maps the ground space to zero. Taking absolute values and bounding the trace by the operator norm gives (7.1.4). The full derivation appears in [10].

The error bound depends on $H(s)$ only through the commutator $[P', (H - \lambda_0)^+]$ and its derivative. The following bounds express these in terms of the Hamiltonian derivatives $H'$, $H''$ and the spectral gap $g$.

**Lemma 7.1.2** (Projector derivative bounds [10])**.** *Under the conditions of Lemma 7.1.1:*

$$\|P'(s)\| \le \frac{2\|H'(s)\|}{g(s)}, \tag{7.1.5}$$

$$\left\| \left[P'(s),\, (H(s) - \lambda_0(s))^+\right] \right\| \le \frac{4\|H'(s)\|}{g(s)^2}, \tag{7.1.6}$$

$$\left\| \left[P'(s),\, (H(s) - \lambda_0(s))^+\right]' \right\| \le \frac{40\|H'(s)\|^2}{g(s)^3} + \frac{4\|H''(s)\|}{g(s)^2}. \tag{7.1.7}$$

*Proof of (7.1.5).* Let $\Gamma$ be a circle in the complex plane centered at $\lambda_0(s)$ with radius $g(s)/2$. The Riesz integral representation of the projector gives

$$P(s) = \frac{1}{2\pi i} \oint_\Gamma R_{H(s)}(z)\, dz, \tag{7.1.8}$$

where $R_{H(s)}(z) = (zI - H(s))^{-1}$ is the resolvent. Differentiating with respect to $s$:

$$P'(s) = \frac{1}{2\pi i} \oint_\Gamma R_{H(s)}(z)\, H'(s)\, R_{H(s)}(z)\, dz, \tag{7.1.9}$$

using the resolvent identity $R_H' = R_H H' R_H$. On the contour $\Gamma$, every point $z$ lies at distance exactly $g(s)/2$ from $\lambda_0(s)$ and at distance at least $g(s)/2$ from every other eigenvalue (since the nearest eigenvalue is $\lambda_1(s)$ at distance $g(s)$ from $\lambda_0(s)$). Therefore $\|R_{H(s)}(z)\| = 1/\mathrm{dist}(z, \sigma(H(s))) \le 2/g(s)$ on $\Gamma$. Bounding the integral:

$$\|P'(s)\| \le \frac{1}{2\pi} \oint_\Gamma \|R_H(z)\| \cdot \|H'(s)\| \cdot \|R_H(z)\|\, |dz| \le \frac{1}{2\pi} \left(\frac{2}{g}\right)^2 \|H'\| \cdot \pi g = \frac{2\|H'\|}{g}. \tag{7.1.10}$$

□

Bound (7.1.6) follows from (7.1.5): the commutator satisfies $\|[P', (H-\lambda_0)^+]\| \le 2\|P'\| \cdot \|(H-\lambda_0)^+\| \le 2 \cdot 2\|H'\|/g \cdot 1/g = 4\|H'\|/g^2$. Bound (7.1.7) requires additionally the pseudoinverse derivative formula $(H^+)' = -H^+H'H^+ + P'H^+ + H^+P'$ and the second Riesz integral for $P''$; the details appear in [10]. The key structure is that every factor of $H'$ or $H''$ comes with an inverse power of $g$, reflecting the amplification of non-adiabatic transitions by a small spectral gap.

Substituting the derivative bounds into the error bound (7.1.4) with a constant schedule $K'(s) = T$ (so that $(1/K')' = 0$) gives the constant-rate baseline.

**Theorem 7.1.3** (Constant-rate runtime)**.** *Under the conditions of Lemma 7.1.1, a constant schedule $K'(s) = T$ achieves error at most $\varepsilon$ provided*

$$T \ge \frac{1}{\varepsilon} \left( \frac{4\|H'(1)\|}{g(1)^2} + \int_0^1 \frac{40\|H'(s)\|^2}{g(s)^3}\, ds + \int_0^1 \frac{4\|H''(s)\|}{g(s)^2}\, ds \right). \tag{7.1.11}$$

*Proof.* With constant $K'$, the third term in (7.1.4) vanishes. Substituting bounds (7.1.6) and (7.1.7) into the remaining two terms:

$$\varepsilon \le \frac{1}{T} \left( \frac{4\|H'(1)\|}{g(1)^2} + \int_0^1 \frac{40\|H'(s)\|^2}{g(s)^3}\, ds + \int_0^1 \frac{4\|H''(s)\|}{g(s)^2}\, ds \right). \tag{7.1.12}$$

Setting the right side equal to $\varepsilon$ and solving for $T$ gives (7.1.11). □

For the adiabatic Hamiltonian $H(s) = -(1-s)\,|\psi_0\rangle\langle\psi_0| + sH_z$, the derivative $H'(s) = |\psi_0\rangle\langle\psi_0| + H_z$ is constant with $\|H'\| = O(1)$, and $H''(s) = 0$. The dominant term in (7.1.11) is $\int_0^1 g(s)^{-3}\,ds$. From the gap profile of Theorem 6.3.1, the crossing window contributes

$$\int_{s^*-\delta_s}^{s^*+\delta_s} g(s)^{-3}\,ds \geq \frac{2\delta_s}{g_{\min}^3} = \frac{2A_2}{A_1(A_1+1)} \cdot g_{\min}^{-2}, \tag{7.1.13}$$

using $\delta_s = A_2 g_{\min}/(A_1(A_1+1))$ from Eq. (5.4.10). This gives $T_{\text{constant}} = O(\delta_s/(\varepsilon\, g_{\min}^3))$.

For the running example ($M = 2$, $g_{\min} = 1/\sqrt{N}$), the exact gap $g(s) = \sqrt{(2s-1)^2 + 4s(1-s)/N}$ (Eq. (5.3.15)) satisfies $\int_0^1 g(s)^{-3}\,ds = O(N)$ since the integral is dominated by the $O(1/\sqrt{N})$ window where $g \approx 1/\sqrt{N}$. Therefore $T_{\text{constant}} = O(N/\varepsilon)$, matching the classical search complexity. A constant-rate adiabatic schedule provides no quantum speedup. The algorithm wastes time far from the crossing, where the gap is $O(1)$ and fast evolution would suffice, while still moving too quickly near $s^*$ to maintain ground-state fidelity.

## 7.2 The Adaptive Schedule

The constant schedule's failure stems from treating all values of $s$ equally. The error bound (7.1.4) indicates a remedy: make $K'(s)$ large where $g(s)$ is large (slow evolution, low error contribution per unit of $s$) and small where $g(s)$ is small (fast physical evolution, but over a narrow interval of $s$). The natural ansatz is $K'(s)$ proportional to $1/g(s)^p$ for some parameter $p \geq 1$: the schedule slows by a factor of $g^{-p}$ near the gap minimum. The total runtime becomes $T \propto \int_0^1 g(s)^{-p}\,ds$, and the error terms involve $\int g^{q-3}\,ds$ for various $q$ depending on $p$.

The parameter $p$ controls the trade-off between error reduction and runtime. Larger $p$ slows the schedule more aggressively near the crossing, reducing the error but increasing $T$ since more time is spent in the window. The optimal $p$ depends on the gap profile. For profiles where the gap decreases linearly to a minimum — exactly the structure established by Theorem 6.3.1 — any $p \in (1,2)$ balances the integrals. The specific choice affects only the constants, not the asymptotic scaling.

The adaptive rate theorem, extending the eigenpath traversal framework of [15] to the continuous-time setting, formalizes this trade-off.

**Theorem 7.2.1** (Adaptive rate [10])**.** *Let $H(s)$ satisfy the conditions of Lemma 7.1.1, and let $g_0 : [0,1] \to \mathbb{R}^+$ be an absolutely continuous function satisfying $g_0(s) \leq g(s)$ for all $s$. Suppose there exist $1 < p < 2$ and constants $B_1, B_2 \geq 1$ such that*

$$\int_0^1 \frac{ds}{g_0(s)^p} \leq B_1\, g_{\min}^{1-p} \qquad \text{and} \qquad \int_0^1 \frac{ds}{g_0(s)^{3-p}} \leq B_2\, g_{\min}^{p-2}. \tag{7.2.1}$$

*Define*

$$c = \sup_{s\in[0,1]} \left(4\|H'(s)\| + 40\|H'(s)\|^2 B_2 + 4\|H''(s)\| + 6p\,|g_0'(s)|\,\|H'(s)\|\,B_2\right). \tag{7.2.2}$$

*Then the schedule*

$$K'(s) = \frac{1}{\varepsilon} \cdot \frac{c}{g_0(s)^p \cdot g_{\min}^{2-p}} \tag{7.2.3}$$

*achieves error at most $\varepsilon$, with total runtime*

$$T = \int_0^1 K'(s)\,ds \leq \frac{c\,B_1}{\varepsilon\, g_{\min}}. \tag{7.2.4}$$

*Proof.* Let $\varepsilon_0$ denote the actual error. Substituting (7.2.3) into the error bound (7.1.4): $(K')^{-1} = \varepsilon\, g_0^p\, g_{\min}^{2-p}/c$, and $|((K')^{-1})'| = (\varepsilon\, g_{\min}^{2-p}/c) \cdot p\, g_0^{p-1}\,|g_0'|$. The three terms become

$$\varepsilon_0 \leq \frac{\varepsilon}{c}\, g_{\min}^{2-p} \left( g_0(1)^p \left\| \left[P'(1), (H(1)-\lambda_0(1))^+\right] \right\| + \int_0^1 g_0^p \left\| \left[P', (H-\lambda_0)^+\right]' \right\| ds + \int_0^1 p\, g_0^{p-1} |g_0'| \left\| \left[P', (H-\lambda_0)^+\right] \right\| ds \right). \tag{7.2.5}$$

**Boundary term.** Using bound (7.1.6) with $g_0 \leq g$:

$$g_{\min}^{2-p}\, g_0(1)^p \cdot \frac{4\|H'(1)\|}{g(1)^2} \leq 4\|H'(1)\|\, g_{\min}^{2-p}\, g_0(1)^{p-2} \leq 4\|H'\|, \tag{7.2.6}$$

since $g_0 \geq g_{\min}$ and $p \leq 2$ imply $g_0^{p-2} \leq g_{\min}^{p-2}$.

**Commutator derivative integral.** Using bound (7.1.7) and splitting:

$$g_{\min}^{2-p} \int_0^1 g_0^p \cdot \frac{40\|H'\|^2}{g^3}\, ds \leq 40\|H'\|^2\, g_{\min}^{2-p} \int_0^1 \frac{ds}{g_0^{3-p}} \leq 40\|H'\|^2 B_2, \tag{7.2.7}$$

where $g_0^p/g^3 \leq g_0^p/g_0^3 = 1/g_0^{3-p}$ since $g_0 \leq g$, and the $B_2$ condition (7.2.1) absorbs $g_{\min}^{2-p} \cdot g_{\min}^{p-2} = 1$. Similarly, the $H''$ sub-term contributes

$$g_{\min}^{2-p} \int_0^1 g_0^p \cdot \frac{4\|H''\|}{g^2}\, ds \leq 4\|H''\|\, g_{\min}^{2-p} \int_0^1 \frac{ds}{g_0^{2-p}} \leq 4\|H''\|, \tag{7.2.8}$$

since $\int g_0^{p-2}\, ds \leq g_{\min}^{p-2}$ (the integrand is at most $g_{\min}^{p-2}$).

**Schedule variation integral.** Using bound (7.1.6):

$$\begin{aligned} g_{\min}^{2-p} \int_0^1 p\, g_0^{p-1} |g_0'| \cdot \frac{4\|H'\|}{g^2}\, ds &\leq 4p\, \|H'\|\, g_{\min}^{2-p} \int_0^1 \frac{g_0^{p-1}\, |g_0'|}{g_0^2}\, ds \\ &= 4p\, \|H'\|\, g_{\min}^{2-p} \int_0^1 g_0^{p-3}\, |g_0'|\, ds. \end{aligned} \tag{7.2.9}$$

For piecewise linear $g_0$, the derivative $|g_0'|$ is constant on each piece, so $\int g_0^{p-3} |g_0'|\, ds \leq \sup |g_0'| \cdot \int g_0^{p-3}\, ds \leq \sup |g_0'| \cdot B_2\, g_{\min}^{p-2}$. The resulting bound is $4p \sup |g_0'|\, \|H'\|\, B_2$. The constant $c$ in (7.2.2) uses the factor $6p$ rather than $4p$, following the paper's convention [10]; this is a valid overestimate that simplifies the expression without affecting the asymptotic result.

**Collecting.** Summing all contributions:

$$\varepsilon_0 \leq \frac{\varepsilon}{c} \left(4\|H'\| + 40\|H'\|^2 B_2 + 4\|H''\| + 6p\, |g_0'|\, \|H'\|\, B_2\right) \leq \frac{\varepsilon}{c} \cdot c = \varepsilon. \tag{7.2.10}$$

**Runtime.** The total evolution time is

$$T = \int_0^1 K'\, ds = \frac{c}{\varepsilon}\, g_{\min}^{p-2} \int_0^1 \frac{ds}{g_0^p} \leq \frac{c}{\varepsilon}\, g_{\min}^{p-2} \cdot B_1\, g_{\min}^{1-p} = \frac{c\, B_1}{\varepsilon\, g_{\min}}. \tag{7.2.11}$$

□

The error has three contributions: a boundary term that depends on $g_0(1)$ and is $O(1)$; an integral that pairs $g_0^p$ from the schedule with $g^{-3}$ from the derivative bounds, producing $\int g_0^{p-3}\, ds$; and a schedule variation term from the non-constant $K'$. The parameter $p$ balances the two integrals: $B_1$ bounds $\int g_0^{-p}\, ds$ (the runtime cost), while $B_2$ bounds $\int g_0^{p-3}\, ds$ (the error cost). Their product with $g_{\min}^{-1}$ gives the final runtime.

**Corollary 7.2.2.** *If $\int_0^1 g(s)^{-p}\, ds = O(g_{\min}^{1-p})$ for all $p > 1$, and $\|H'\|$, $\|H''\|$, $|\lambda_0'|$, $|g'|$ are all $O(1)$, then $T = O(1/(\varepsilon\, g_{\min}))$.*

The runtime scales inversely with the minimum gap, which is optimal for quantum search [2]. The running example satisfies these conditions.

**Lemma 7.2.3** (Grover gap integral)**.** *For the exact gap $g(s) = \sqrt{(2s-1)^2 + 4s(1-s)/N}$ of the running example ($M = 2$, $d_0 = 1$, $d_1 = N - 1$),*

$$\int_0^1 g(s)^{-p}\, ds = O\left(N^{(p-1)/2}\right) = O\left(g_{\min}^{1-p}\right) \qquad \text{for all } p > 1. \tag{7.2.12}$$

*Proof.* The gap is symmetric about $s = 1/2$ and achieves its minimum $g_{\min} = 1/\sqrt{N}$ there. Split the integral at $1/2 - 1/\sqrt{N}$. In the window $[1/2 - 1/\sqrt{N},\, 1/2]$, bound $g \geq g_{\min}$:

$$\int_{1/2-1/\sqrt{N}}^{1/2} g^{-p}\, ds \leq \frac{1}{\sqrt{N}} \cdot N^{p/2} = N^{(p-1)/2}. \tag{7.2.13}$$

Outside the window, $g(s) \geq c|s - 1/2|$ for a constant $c > 0$ (the gap grows linearly away from the minimum). The change of variable $u = g(s)$, with $|ds/du| = O(1)$ since $|g'(s)| \leq 2$, gives

$$\int_0^{1/2-1/\sqrt{N}} g^{-p}\, ds \leq C \int_{1/\sqrt{N}}^{O(1)} u^{-p}\, du = O\left(N^{(p-1)/2}\right). \tag{7.2.14}$$

Combining and using the symmetry about $1/2$ gives the result. □

The other conditions of Corollary 7.2.2 are immediate: $\|H'\| = \||\psi_0\rangle\langle\psi_0| + H_z\| \le 2$, $H'' = 0$, $|\lambda_0'| \le \|H'\| \le 2$ by the Hellmann-Feynman theorem, and $|g'(s)| \le 2$ (from $|g'| = |4(1-1/N)(1/2-s)/g| \le 2$, since the numerator is at most $2g$). Therefore $T = O(\sqrt{N}/\varepsilon)$ for the running example with an adaptive schedule, compared to $T = O(N/\varepsilon)$ with a constant schedule. The adaptive schedule recovers the full Grover speedup.

The schedule $K'(s) \propto 1/g(s)^p$ concentrates the evolution time near the crossing: at $s = 1/2$, where $g \approx 1/\sqrt{N}$, the schedule rate is $K' \propto N^{p/2}$, while far from $1/2$, where $g = O(1)$, it is $K' = O(1)$. The algorithm spends $O(\sqrt{N})$ physical time traversing the window and $O(1)$ time traversing the rest of $[0,1]$.

## 7.3 Runtime of Adiabatic Quantum Optimization

Applying Theorem 7.2.1 to the adiabatic Hamiltonian $H(s) = -(1-s)|\psi_0\rangle\langle\psi_0| + sH_z$ with the gap profile of Theorem 6.3.1 requires three steps: construct a continuous lower bound $g_0(s)$ from the piecewise bounds, compute $B_1$ and $B_2$, and evaluate the constant $c$.

The piecewise bounds of Theorem 6.3.1 are valid in their respective regions but are not continuous at the boundaries $s^* - \delta_s$ and $s^*$: the left bound exceeds the window bound at $s^* - \delta_s$, and the right bound is smaller than $g_{\min}$ at $s^*$. The adaptive rate theorem requires $g_0$ to be absolutely continuous on $[0,1]$. Shrinking the left and window bounds by a constant factor $b$ makes all three pieces meet continuously at the boundaries.

Define

$$g_0(s) = \begin{cases} b\,\dfrac{A_1(A_1+1)}{A_2}\,(s^* - s)\,, & s \in [0,\, s^* - \delta_s), \\ b\,g_{\min}, & s \in [s^* - \delta_s,\, s^*), \\ \dfrac{\Delta}{30}\cdot\dfrac{s - s_0}{1 - s_0}, & s \in [s^*,\, 1], \end{cases} \tag{7.3.1}$$

where $s_0$ is given by Eq. (6.2.5) and the shrinking factor is

$$b = k \cdot \frac{2}{1 + f(s^*)} = \frac{1}{4}\cdot\frac{2}{1+4} = \frac{1}{10}, \tag{7.3.2}$$

using $k = 1/4$ and $f(s^*) = 4$ from Eq. (6.2.23).

Each piece of $g_0$ lies below the corresponding gap bound from Theorem 6.3.1: the left and window pieces are shrunk by $b = 1/10$, and the right piece equals the original bound. The function $g_0$ is continuous at both boundaries. At $s = s^* - \delta_s$, the left piece gives $b \cdot A_1(A_1+1)\delta_s/A_2$. Using $\delta_s = A_2 g_{\min}/(A_1(A_1+1))$ from Eq. (5.4.10), this equals $b\,g_{\min} = g_{\min}/10$, matching the window piece. At $s = s^*$, the window piece gives $b\,g_{\min} = g_{\min}/10$, and the right piece gives $(\Delta/30)(s^* - s_0)/(1 - s_0)$. Using $s^* - s_0 = k\,g_{\min}(1-s^*)/(a - k\,g_{\min})$ and $1 - s_0 = (1-s^*)\cdot a/(a - k\,g_{\min})$ from Eq. (6.2.5):

$$\frac{\Delta}{30}\cdot\frac{s^* - s_0}{1 - s_0} = \frac{\Delta}{30}\cdot\frac{k\,g_{\min}}{a} = \frac{\Delta}{30}\cdot\frac{g_{\min}/4}{\Delta/12} = \frac{g_{\min}}{10}, \tag{7.3.3}$$

again matching the window piece. The parameters $b$, $k$, and $a$ are coupled precisely so that $g_0$ is continuous: the shrinking factor $b = 1/10$ absorbs both the ratio $k = 1/4$ from the right-side resolvent bound and the value $f(s^*) = 4$ from the monotonicity analysis of Chapter 6.

The integral $\int_0^1 g_0^{-p}\,ds$ splits across the three regions. In the left region, $g_0(s) = b\,A_1(A_1+1)(s^* - s)/A_2$, so

$$\begin{aligned} \int_0^{s^*-\delta_s} g_0^{-p}\,ds &= \left(\frac{A_2}{b\,A_1(A_1+1)}\right)^p \int_{\delta_s}^{s^*} \frac{du}{u^p} = \frac{1}{b^p}\left(\frac{A_2}{A_1(A_1+1)}\right)^p \cdot \frac{1}{(p-1)\,\delta_s^{p-1}} \\ &= \frac{1}{b^p(p-1)}\cdot\frac{A_2}{A_1(A_1+1)}\cdot g_{\min}^{1-p}, \end{aligned} \tag{7.3.4}$$

where the last step uses $\delta_s^{p-1} = (A_2 g_{\min}/(A_1(A_1+1)))^{p-1}$. In the window, $g_0 = b\,g_{\min}$ is constant:

$$\int_{s^*-\delta_s}^{s^*} g_0^{-p}\,ds = \frac{\delta_s}{b^p\,g_{\min}^p} = \frac{1}{b^p}\cdot\frac{A_2}{A_1(A_1+1)}\cdot g_{\min}^{1-p}. \tag{7.3.5}$$

Combining the left and window contributions with $b^{-p} = 10^p$: $(1/(p-1) + 1)/b^p = p\cdot 10^p/(p-1)$, giving $(p/(p-1))\cdot 10^p \cdot A_2/(A_1(A_1+1))\cdot g_{\min}^{1-p}$.

In the right region, $g_0(s) = (\Delta/30)(s - s_0)/(1 - s_0)$, so

$$\int_{s^*}^{1} g_0^{-p}\, ds = \left(\frac{30(1-s_0)}{\Delta}\right)^p \int_{s^*-s_0}^{1-s_0} \frac{du}{u^p} = \left(\frac{30(1-s_0)}{\Delta}\right)^p \cdot \frac{1}{(p-1)(s^*-s_0)^{p-1}}$$
$$= \frac{1}{p-1}\left(\frac{30}{\Delta}\right)^p \left(\frac{a}{k}\right)^{p-1} (1-s_0)\cdot g_{\min}^{1-p}, \tag{7.3.6}$$

using $s^* - s_0 = k\, g_{\min}(1 - s^*)/(a - k\, g_{\min})$ and $1 - s_0 = a(1 - s^*)/(a - k\, g_{\min})$. With $a = (4/3)k^2\Delta$ and $k = 1/4$: $a/k = \Delta/3$, so $(30/\Delta)^p(\Delta/3)^{p-1} = 30^p/(3\Delta)$, and $(1 - s_0) \le 1/(1 + A_1)$. The right contribution is $3 \cdot 10^p/((p-1)\Delta(1 + A_1)) \cdot g_{\min}^{1-p}$.

Since $\Delta A_2 \le A_1$ (from $A_2 \le A_1/\Delta$, which follows because $A_2 = (1/N)\sum d_k/(E_k - E_0)^2 \le (1/\Delta) \cdot (1/N)\sum d_k/(E_k - E_0) = A_1/\Delta$), the left-plus-window term $A_2/(A_1(1 + A_1)) \le 1/(\Delta(1 + A_1))$. Combining all three:

$$\int_0^1 g_0^{-p}\, ds \le \frac{(p+3)\cdot 10^p}{(p-1)(1+A_1)\Delta} \cdot g_{\min}^{1-p}, \qquad \text{so} \quad B_1 = O\left(\frac{1}{\Delta(1+A_1)}\right). \tag{7.3.7}$$

The integral $\int_0^1 g_0^{p-3}\, ds$ has the same three-region structure, with the exponent $p$ replaced by $3 - p$. Since $3 - p \in (1, 2)$, the integrals converge and evaluate by the same substitutions, giving

$$B_2 = O\left(\frac{1}{\Delta(1+A_1)}\right). \tag{7.3.8}$$

For the adiabatic Hamiltonian $H(s) = -(1 - s)\,|\psi_0\rangle\langle\psi_0| + sH_z$:

$$\|H'(s)\| = O(1), \qquad \|H''(s)\| = 0, \qquad |\lambda_0'(s)| = O(1), \tag{7.3.9}$$

since $H'(s) = |\psi_0\rangle\langle\psi_0| + H_z$ is constant and $\lambda_0'(s) = \langle\phi_0(s)|\, H'(s)\, |\phi_0(s)\rangle$ is bounded by $\|H'\|$ via the Hellmann-Feynman theorem. The derivative $|g_0'(s)|$ is bounded on each piece: on the left, $|g_0'| = b\, A_1(A_1 + 1)/A_2$; in the window, $g_0' = 0$; on the right, $|g_0'| = \Delta/(30(1 - s_0))$. For piecewise linear $g_0$, the product $|g_0'| \cdot B_2$ remains bounded because the integral $\int g_0^{p-3}|g_0'|\, ds = \int g_0^{p-3}\, dg_0 = O(g_{\min}^{p-2})$ by change of variable, independently of the slopes. Therefore

$$c = O(B_2). \tag{7.3.10}$$

**Theorem 7.3.1** (Runtime of AQO — Main Result 1 [10])**.** *Let $H_z$ satisfy the spectral condition (Definition 5.2.2). For any $\varepsilon > 0$, the adaptive schedule (7.2.3) with the gap lower bound (7.3.1) prepares the ground state of $H_z$ with fidelity at least $1 - \varepsilon$ in time*

$$T = O\left(\frac{1}{\varepsilon} \cdot \frac{\sqrt{A_2}}{\Delta^2\, A_1(A_1+1)} \cdot \sqrt{\frac{N}{d_0}}\right). \tag{7.3.11}$$

*Proof.* By Theorem 7.2.1, $T \le c\, B_1/(\varepsilon\, g_{\min})$. Substituting $c = O(B_2)$, $B_1 = O(1/(\Delta(1 + A_1)))$, $B_2 = O(1/(\Delta(1 + A_1)))$, and $g_{\min} = (2A_1/(A_1 + 1))\sqrt{d_0/(NA_2)}$ from Eq. (5.4.9):

$$T = O\left(\frac{1}{\varepsilon} \cdot \frac{B_1 B_2}{g_{\min}}\right) = O\left(\frac{1}{\varepsilon} \cdot \frac{1}{\Delta^2(1+A_1)^2} \cdot \frac{A_1+1}{2A_1}\sqrt{\frac{NA_2}{d_0}}\right) = O\left(\frac{1}{\varepsilon} \cdot \frac{\sqrt{A_2}}{\Delta^2\, A_1(A_1+1)} \cdot \sqrt{\frac{N}{d_0}}\right). \tag{7.3.12}$$

□

The runtime (7.3.11) decomposes into five factors. The dependence $1/\varepsilon$ is linear in the target precision: the adaptive schedule converts time directly into fidelity, unlike the standard adiabatic theorem where $T$ scales as $1/\varepsilon$ times a higher polynomial in $1/g_{\min}$. The factor $\sqrt{A_2}$ reflects the spectral spread: larger $A_2 = (1/N)\sum d_k/(E_k - E_0)^2$ means eigenvalues close to $E_0$ carry substantial degeneracy, sharpening the gap minimum and narrowing the crossing window. The denominator $A_1(A_1 + 1)$ captures the crossing position: larger $A_1$ pushes $s^*$ closer to 1, steepening the gap's left arm and allowing faster traversal. The factor $1/\Delta^2$ is the price of the right-side bound — a larger spectral gap $\Delta$ in $H_z$ means the gap reopens faster after the crossing, and the quadratic dependence arises because both $B_1$ and $B_2$ contribute a factor of $1/\Delta$. The dominant factor $\sqrt{N/d_0}$ is the quantum speedup: $\sqrt{N} = \sqrt{2^n}$ is exponential in $n$, and more solutions (larger $d_0$) reduce the runtime.

For the Ising Hamiltonian $H_\sigma$ (Eq. (5.1.4)) with $A_1, A_2 = O(\mathrm{poly}(n))$ and $\Delta \ge 1/\mathrm{poly}(n)$: $T = \widetilde{O}(\sqrt{N/d_0})$, matching the lower bound of [2] up to polylogarithmic factors. When $d_0 = O(1)$ (constant number of solutions), the adiabatic algorithm achieves the Grover speedup $\sqrt{N}$.

For the running example ($M = 2$, $A_1 = (N-1)/N \approx 1$, $A_2 = (N-1)/N \approx 1$, $\Delta = 1$, $d_0 = 1$):

$$T = O\left(\frac{1}{\varepsilon} \cdot \frac{1}{1 \cdot 2} \cdot \sqrt{N}\right) = O\left(\frac{\sqrt{N}}{\varepsilon}\right), \tag{7.3.13}$$

matching the circuit-based Grover algorithm. The adaptive adiabatic approach achieves the same quadratic speedup through a smooth interpolation between two Hamiltonians, without requiring oracle queries or amplitude amplification.

The result comes with a caveat. The schedule (7.2.3) requires knowing $g_0(s)$, which requires knowing $s^*$, $\delta_s$, and $g_{\min}$. All three depend on the spectral parameter $A_1$. In the crossing window $[s^* - \delta_s, s^*)$, the schedule is constant: $K' = c/(\varepsilon\, b^p\, g_{\min}^2)$. This rate does not depend on $A_1$ beyond $g_{\min}$. But the window's location is $[s^* - \delta_s, s^*)$, and $s^* = A_1/(A_1 + 1)$ must be known to accuracy $O(\delta_s) = O(2^{-n/2})$ to ensure the slow phase occurs at the right place. Outside the window, the schedule depends linearly on the distance from $s^*$, so a small error in $s^*$ introduces a proportionally small error in $K'$, absorbed by the polynomial factors. But the window itself is exponentially narrow in $n$: placing it incorrectly causes the algorithm to evolve rapidly through the crossing, destroying the ground-state fidelity.

The parameters $A_2$ and $d_0$ need not be known precisely. Replacing $A_2$ with the constant lower bound 1 (valid for all Hamiltonians with at least two energy levels) and setting $d_0 = 1$ (the worst case) introduces at most a poly$(n)$ slowdown in the runtime, since these parameters enter only through the ratio $\sqrt{A_2/d_0}$ and the bound $B_1$. The critical parameter is $A_1$: it must be computed to additive accuracy $O(\delta_s) = O(2^{-n/2})$ before the evolution begins. How hard is this computation? The precision needed is exponential in $n$, while the problem Hamiltonian $H_z$ is specified by poly$(n)$ bits. Chapter 8 answers this question: approximating $A_1$ to additive accuracy $1/\text{poly}(n)$ — far less precision than needed — is already NP-hard, and computing $A_1$ exactly is #P-hard.

# Chapter 8

# Hardness of Optimality

The optimal schedule of the previous chapter achieves a quadratic speedup over classical brute-force search, but the schedule must be fixed before evolution begins. It depends on the spectral parameter $A_1$ — the weighted sum of inverse gaps that determines where the avoided crossing occurs — and this parameter must be known to additive accuracy $O(2^{-n/2})$. Given the $N = 2^n$ diagonal entries of the problem Hamiltonian $H_z$, the brute-force approach to computing $A_1 = (1/N)\sum_{k=1}^{M-1} d_k/(E_k - E_0)$ — enumerating all eigenvalues, sorting, and summing — takes $O(N)$ time, precisely the cost of classical unstructured search. If the pre-computation is as expensive as the problem itself, the quadratic speedup becomes conditional: the adiabatic algorithm is fast, provided someone has already done the slow part.

The runtime of Theorem 7.3.1,

$$T = O\left(\frac{1}{\varepsilon}\cdot\frac{\sqrt{A_2}}{\Delta^2\, A_1(A_1+1)}\cdot\sqrt{\frac{N}{d_0}}\right),$$

makes this dependence explicit. The adaptive schedule places a slow phase in the window $[s^*-\delta_s,\, s^*)$ centered at the crossing position $s^* = A_1/(A_1+1)$, where the spectral gap reaches its minimum, and accelerates elsewhere. The parameters $A_2$ and $d_0$ enter only through the ratio $\sqrt{A_2/d_0}$ and can be replaced by conservative bounds ($A_2 \geq 1$, $d_0 = 1$) at the cost of polynomial slowdown. The critical parameter is $A_1$: it determines where the crossing occurs, and the window width $\delta_s = O(\sqrt{d_0/(NA_2)}) = O(2^{-n/2})$ sets the required precision. An error larger than $\delta_s$ in the crossing position causes the algorithm to evolve rapidly through the gap minimum, destroying the ground-state fidelity. Throughout this chapter, we write $A_1(H)$ to make the dependence on the Hamiltonian explicit when multiple Hamiltonians are under consideration.

Estimating $A_1$ to the much coarser precision $1/\mathrm{poly}(n)$ is already NP-hard: two queries to an $A_1$-oracle suffice to solve 3-SAT (section 8.1). Computing $A_1$ exactly, or to exponentially small precision $O(2^{-\mathrm{poly}(n)})$, is #P-hard: polynomial interpolation extracts all degeneracies $d_k$ from polynomially many queries (section 8.2). At the algorithmically relevant precision $2^{-n/2}$, the interpolation technique breaks down, but a quantum algorithm achieves $O(2^{n/2})$ queries while any classical algorithm requires $\Omega(2^n)$, yielding a Grover-type quadratic separation (section 8.3).

## 8.1 NP-Hardness of Estimating $A_1$

The Hamiltonian $H_z$ encodes an optimization problem whose ground energy $E_0$ determines whether a solution exists. For a 3-SAT instance, $E_0 = 0$ when a satisfying assignment exists and $E_0 \geq 1/\mathrm{poly}(n)$ otherwise. Distinguishing these two cases is the local Hamiltonian promise problem, known to be NP-hard [16]. The spectral parameter $A_1$ is not obviously related to this decision problem — it aggregates information about all energy levels, not just the ground energy. A modified Hamiltonian $H'$ creates a bridge: comparing $A_1(H')$ with $A_1(H)$ reveals whether $E_0$ vanishes.

Define the $(n+1)$-qubit Hamiltonian

$$H' = H \otimes \frac{I+\sigma_z}{2}. \tag{8.1.1}$$

The operator $(I+\sigma_z)/2$ is the projector onto $|0\rangle$ for the ancilla qubit: it has eigenvalue 1 on $|0\rangle$ and eigenvalue 0 on $|1\rangle$. On the $|0\rangle$ branch, $H'$ has the same spectrum as $H$: eigenvalues $E_k$ with degeneracies $d_k$. On the $|1\rangle$ branch, $H'$ annihilates every state, contributing $2^n$ eigenvalues at energy 0. The ground energy of $H'$ is therefore always zero, regardless of $E_0(H)$. This invariance is the mechanism: $A_1(H')$ measures the spectrum from a

fixed reference point $E_0' = 0$, while $A_1(H)$ measures from the variable reference $E_0(H)$. When $E_0(H) > 0$, the two measurements diverge, and the divergence is detectable.

**Lemma 8.1.1** (Disambiguation [10]). *Let $\varepsilon, \mu_1, \mu_2 \in (0,1)$. Suppose $\mathcal{C}_\varepsilon$ is a procedure that accepts the description of a Hamiltonian $H$ and outputs $\widetilde{A}_1(H)$ with $|\widetilde{A}_1(H) - A_1(H)| \le \varepsilon$. Let $H$ be an $n$-qubit diagonal Hamiltonian with eigenvalues $0 \le E_0 < E_1 < \cdots < E_{M-1} \le 1$ and $M \in \mathrm{poly}(n)$, such that either* (i) $E_0 = 0$ *or* (ii) $\mu_1 \le E_0 \le 1 - \mu_2$. *Then two calls to $\mathcal{C}_\varepsilon$ suffice to decide between* (i) *and* (ii), *provided*

$$\varepsilon < \frac{\mu_1}{6(1-\mu_1)} - \frac{d_0}{6N} \cdot \frac{1}{\mu_1 \mu_2}. \tag{8.1.2}$$

*Proof.* Call $\mathcal{C}_\varepsilon$ on $H$ and on $H'$ defined by Eq. (8.1.1), obtaining estimates $\widetilde{A}_1(H)$ and $\widetilde{A}_1(H')$. The test statistic is $\widetilde{A}_1(H) - 2\widetilde{A}_1(H')$, where the factor 2 compensates for the doubling of the Hilbert space ($H'$ acts on $2^{n+1}$ states, so $A_1(H')$ carries a normalization factor $1/2^{n+1}$ instead of $1/2^n$).

**Case (i): $E_0 = 0$.** The ground energy of $H'$ is 0 with degeneracy $d_0 + 2^n$, and the excited levels of $H'$ are $E_1, \ldots, E_{M-1}$ with degeneracies $d_1, \ldots, d_{M-1}$. Since $E_0 = 0$, both $A_1(H)$ and $A_1(H')$ sum over the same gaps $E_k - 0 = E_k$:

$$A_1(H) = \frac{1}{2^n} \sum_{k=1}^{M-1} \frac{d_k}{E_k}, \qquad A_1(H') = \frac{1}{2^{n+1}} \sum_{k=1}^{M-1} \frac{d_k}{E_k}.$$

Therefore $A_1(H) - 2A_1(H') = 0$, and by the triangle inequality the test statistic satisfies $|\widetilde{A}_1(H) - 2\widetilde{A}_1(H')| \le 3\varepsilon$.

**Case (ii): $\mu_1 \le E_0 \le 1 - \mu_2$.** The ground energy of $H'$ is still 0 (from the $|1\rangle$ branch), but now $E_0, E_1, \ldots, E_{M-1}$ are all excited levels. Thus

$$A_1(H') = \frac{1}{2^{n+1}} \sum_{k=0}^{M-1} \frac{d_k}{E_k}.$$

Decompose $A_1(H)$ using the partial fraction identity $d_k/(E_k - E_0) = d_k/E_k + d_k E_0/(E_k(E_k - E_0))$:

$$\begin{aligned} A_1(H) &= \frac{1}{2^n} \sum_{k=1}^{M-1} \frac{d_k}{E_k - E_0} = \frac{1}{2^n} \sum_{k=1}^{M-1} \frac{d_k}{E_k} + \frac{E_0}{2^n} \sum_{k=1}^{M-1} \frac{d_k}{E_k(E_k - E_0)} \\ &= \frac{1}{2^n} \sum_{k=0}^{M-1} \frac{d_k}{E_k} - \frac{d_0}{2^n E_0} + \frac{E_0}{2^n} \sum_{k=1}^{M-1} \frac{d_k}{E_k(E_k - E_0)}. \end{aligned} \tag{8.1.3}$$

The first sum equals $2A_1(H')$. For the remainder sum, $E_k \le 1$ and $E_k - E_0 \le 1 - E_0$, so the product $E_k(E_k - E_0)$ is at most $1 - E_0$. Each fraction $d_k/(E_k(E_k - E_0))$ is therefore bounded from below:

$$\frac{E_0}{2^n} \sum_{k=1}^{M-1} \frac{d_k}{E_k(E_k - E_0)} \ge \frac{E_0}{1 - E_0} \cdot \frac{1}{2^n} \sum_{k=1}^{M-1} d_k = \frac{E_0}{1 - E_0} \left(1 - \frac{d_0}{N}\right).$$

Combining with Eq. (8.1.3):

$$\begin{aligned} A_1(H) - 2A_1(H') &\ge \frac{E_0}{1 - E_0} \left(1 - \frac{d_0}{N}\right) - \frac{d_0}{N E_0} \\ &= \frac{E_0}{1 - E_0} - \frac{d_0}{N} \cdot \frac{1 - E_0 + E_0^2}{E_0(1 - E_0)}. \end{aligned} \tag{8.1.4}$$

Since $1 - E_0 + E_0^2 \le 1$ and $E_0(1 - E_0) \ge \mu_1 \mu_2$ on the given range, the fraction $(1 - E_0 + E_0^2)/(E_0(1 - E_0))$ is at most $1/(\mu_1 \mu_2)$. The first term $E_0/(1 - E_0)$ is increasing in $E_0$, so it is at least $\mu_1/(1 - \mu_1)$. Therefore

$$A_1(H) - 2A_1(H') \ge \frac{\mu_1}{1 - \mu_1} - \frac{d_0}{N} \cdot \frac{1}{\mu_1 \mu_2},$$

and the test statistic satisfies

$$\widetilde{A}_1(H) - 2\widetilde{A}_1(H') \ge \frac{\mu_1}{1 - \mu_1} - \frac{d_0}{N \mu_1 \mu_2} - 3\varepsilon.$$

The two cases are distinguished when $3\varepsilon$ from case (i) is separated from the lower bound in case (ii), requiring $6\varepsilon < \mu_1/(1 - \mu_1) - d_0/(N \mu_1 \mu_2)$. □

The disambiguation succeeds whenever the positive correction $E_0/(1-E_0)$ from the partial fraction identity dominates the negative term $-d_0/(NE_0)$, which happens as long as $d_0/N$ is small relative to $\mu_1^2\mu_2$. For the Ising Hamiltonians of interest, $d_0/N$ is exponentially small in $n$, so the condition is easily satisfied.

**Theorem 8.1.2** (NP-hardness of $A_1$ estimation [10])**.** *Computing $A_1(H)$ to additive accuracy*

$$\varepsilon < \frac{1}{72(n-1)}$$

*for a 3-local Hamiltonian $H$ on $n$ qubits is NP-hard.*

*Proof.* We reduce 3-SAT to ground-energy disambiguation, following the construction of [17, 10]. Let $\varphi$ be a 3-SAT formula on $n_{\text{var}}$ Boolean variables $x_0, \ldots, x_{n_{\text{var}}-1}$ with $m$ clauses, each of the form $a_k \vee b_k \vee c_k$ where each literal is some $x_l$ or $\bar{x}_l$. If $n_{\text{var}} + m < 15$, solve by brute force. Otherwise, define the single-qubit projectors

$$P_{x_l} = \frac{I - \sigma_z^{(l)}}{2}, \qquad P_{\bar{x}_l} = \frac{I + \sigma_z^{(l)}}{2},$$

which project onto the $|1\rangle$ and $|0\rangle$ states of qubit $l$, respectively. For each clause $k$ ($0 \le k < m$), introduce an auxiliary qubit at index $n_{\text{var}} + k$ and define

$$\begin{aligned} H_k = {} & P_{\bar{a}_k} + P_{\bar{b}_k} + P_{\bar{c}_k} + P_{\bar{x}_{n_{\text{var}}+k}} \\ & + P_{a_k}P_{b_k} + P_{a_k}P_{c_k} + P_{b_k}P_{c_k} \\ & + P_{\bar{a}_k}P_{x_{n_{\text{var}}+k}} + P_{\bar{b}_k}P_{x_{n_{\text{var}}+k}} + P_{\bar{c}_k}P_{x_{n_{\text{var}}+k}}. \end{aligned} \tag{8.1.5}$$

Direct computation on the computational basis shows that the minimum eigenvalue of $H_k$ is 3 when clause $k$ is satisfied and 4 when it is not; the maximum eigenvalue is 6. The combined Hamiltonian on $2n_{\text{var}} + 2m$ qubits is

$$H = \frac{1}{6m}\sum_{k=0}^{m-1} H_k + \frac{1}{2n_{\text{var}} + 2m}\sum_{j=n_{\text{var}}+m}^{2n_{\text{var}}+2m-1} P_{x_j} - \frac{1}{2}I. \tag{8.1.6}$$

The first sum normalizes the clause energies to $[1/2, 1]$; the second sum adds $n_{\text{var}} + m$ free qubits whose projectors prefer $|0\rangle$; the identity shift places the eigenvalues in $[0, 1]$. When all clauses are satisfied, there exists an assignment making every $H_k$ achieve its minimum, giving $E_0 = 0$. When some clause is unsatisfied, the minimum of $\sum H_k/(6m)$ increases by at least $1/(6m)$, giving $E_0 \ge 1/(6m)$.

Apply Lemma 8.1.1 with $\mu_1 = 1/(6m)$ and $\mu_2 = 1/2$. The number of eigenvalues is $N = 2^{2n_{\text{var}}+2m}$ and the ground-state degeneracy satisfies $d_0 \le 2^{n_{\text{var}}+m}$, so $d_0/N \le 2^{-(n_{\text{var}}+m)}$. The precision requirement in Eq. (8.1.2) becomes

$$\begin{aligned} \varepsilon &< \frac{1}{6}\cdot\frac{1}{6m-1} - \frac{12m}{6}\cdot\frac{d_0}{N} \\ &\le \frac{1}{36(n_{\text{var}}+m-1)} - \frac{2m}{2^{n_{\text{var}}+m}}. \end{aligned} \tag{8.1.7}$$

For $n_{\text{var}} + m \ge 15$, the second term satisfies $2m/2^{n_{\text{var}}+m} \le 1/(72(n_{\text{var}}+m-1))$, so

$$\varepsilon < \frac{1}{72(n_{\text{var}}+m-1)}.$$

The Hamiltonian $H'$ from Eq. (8.1.1) acts on $n = 2n_{\text{var}} + 2m + 1$ qubits and is 3-local (since $H$ is 2-local and the tensor product with $(I+\sigma_z)/2$ adds one ancilla). Since $n_{\text{var}} + m \le n$, the precision bound $\varepsilon < 1/(72(n-1))$ follows. □

For the running example ($M = 2$, Grover search), the spectral parameter $A_1 = (N-1)/N$ is trivially known from the problem description: there are only two energy levels, and the degeneracies are determined by the number of marked items. The NP-hardness arises from Hamiltonians encoding combinatorial problems with polynomially many energy levels and exponentially small ground-energy gaps, where $A_1$ depends on the full degeneracy structure in a non-trivial way.

**Remark.** The disambiguation technique extends beyond 3-SAT. The MaxCut decision problem — given a graph $G = (V, E)$ and integer $k$, does $G$ have a cut of size at least $k$? — also reduces to $A_1$ estimation. The construction adds a weighted edge to $G$, creating an auxiliary Hamiltonian $H'$ whose $A_1$ value differs from a reference by at least $1/(|E|(|E|-1))$ between the two cases. This yields NP-hardness at precision $2/(5n^4)$ with a 2-local Hamiltonian, sharpening the locality requirement from 3-local to 2-local at the cost of a slightly tighter precision bound.

## 8.2 #P-Hardness of Computing $A_1$ Exactly

NP-hardness captures the decision problem: is $E_0 = 0$? But $A_1$ encodes more than a single bit. The spectral parameter is a weighted sum over all energy levels, and its exact value determines every degeneracy $d_k$. Extracting these degeneracies solves counting problems — $d_0$ for an NP-complete Hamiltonian counts the number of satisfying assignments — and counting is harder than deciding: it is #P-complete [18].

The extraction uses a parametrized family of Hamiltonians that shifts the spectrum continuously, turning $A_1$ into a rational function whose poles carry the degeneracies as residues. For a parameter $x > 0$, define the $(n+1)$-qubit Hamiltonian

$$H'(x) = H \otimes I - \frac{x}{2} I \otimes \frac{I + \sigma_z^{(n+1)}}{2}. \tag{8.2.1}$$

On the $|0\rangle$ branch of the ancilla, the eigenvalues are $E_k - x/2$ with degeneracies $d_k$. On the $|1\rangle$ branch, the eigenvalues are $E_k$ with degeneracies $d_k$. The ground energy is $E_0 - x/2$ (from the $|0\rangle$ branch, for $x > 0$). The gaps relative to this ground energy are $\Delta_k = E_k - E_0$ for the $|0\rangle$ branch and $\Delta_k + x/2$ for the $|1\rangle$ branch.

Computing $A_1(H'(x))$ from these gaps and defining $f(x) = 2A_1(H'(x)) - A_1(H)$ isolates the $|1\rangle$-branch contribution [10]:

$$f(x) = \frac{1}{N} \sum_{k=0}^{M-1} \frac{d_k}{\Delta_k + x/2}. \tag{8.2.2}$$

This function is a sum of $M$ simple poles at $x = -2\Delta_k$. Each pole has residue $2d_k/N$, encoding the degeneracy of the corresponding energy level. The function $f$ is a partial-fraction decomposition of the entire degeneracy spectrum. The extraction problem reduces to recovering these residues from evaluations of $f$.

**Lemma 8.2.1** (Exact degeneracy extraction [10])**.** *Suppose $\mathcal{C}$ is a procedure that computes $A_1(H)$ exactly for any $n$-qubit diagonal Hamiltonian $H$. Let $H_\sigma$ be an Ising Hamiltonian (Equation 5.1.4) with integer eigenvalues and known spectral gaps $\Delta_k = E_k - E_0$. Then $O(\text{poly}(n))$ calls to $\mathcal{C}$ suffice to compute all degeneracies $d_0, d_1, \ldots, d_{M-1}$.*

*Proof.* Each evaluation of $f(x_i)$ requires two calls to $\mathcal{C}$: one for $A_1(H)$ and one for $A_1(H'(x_i))$. Evaluate $f$ at $M$ distinct positive odd integers $x_i \in \{1, 3, \ldots, 2M-1\}$. These values avoid the poles: for each $k$, $\Delta_k + x_i/2 \geq 0 + 1/2 > 0$ since $\Delta_k \geq 0$ and $x_i \geq 1$. The total cost is $2M = O(\text{poly}(n))$ oracle calls.

Define the reconstruction polynomial

$$P(x) = \prod_{k=0}^{M-1} \left(\Delta_k + \frac{x}{2}\right) f(x) = \frac{1}{N} \sum_{k=0}^{M-1} d_k \prod_{\ell \neq k} \left(\Delta_\ell + \frac{x}{2}\right). \tag{8.2.3}$$

Multiplying $f(x)$ by the product of all denominators clears the poles, yielding a polynomial of degree at most $M-1$ in $x$. Since the gaps $\Delta_k$ are known integers, the values $P(x_i) = \prod_k (\Delta_k + x_i/2) \cdot f(x_i)$ are computable from the oracle outputs. The $M$ values $P(x_1), \ldots, P(x_M)$ determine $P$ uniquely by Lagrange interpolation [19]: a polynomial of degree at most $M-1$ is determined by $M$ distinct evaluations.

The degeneracies are recovered by evaluating $P$ at the poles. Setting $x = -2\Delta_k$ kills every factor $(\Delta_\ell + x/2)$ except the $k$-th, giving

$$d_k = \frac{N \cdot P(-2\Delta_k)}{\prod_{\ell \neq k} (\Delta_\ell - \Delta_k)}, \qquad k \in \{0, \ldots, M-1\}. \tag{8.2.4}$$

The denominator is nonzero because the eigenvalues are distinct. The entire computation (oracle calls, Lagrange interpolation, pole evaluation) runs in $O(\text{poly}(n))$ time. □

Extracting $d_0$ from an Ising Hamiltonian encoding a 3-SAT formula counts the number of satisfying assignments, solving #3-SAT. Since #3-SAT is #P-complete [18], an exact $A_1$ oracle would solve every problem in #P in polynomial time. The degeneracies also determine the output probability of an IQP circuit [20]: from the $d_k$ and $\Delta_k$, one computes $|\langle 0^n | C_{\text{IQP}} | 0^n \rangle|^2 = |N^{-1} \sum_k d_k \, e^{i\Delta_k}|^2$, which is itself #P-hard. The NP-hardness of section 8.1 uses a 3-local Hamiltonian (the ancilla qubit raises the locality by one). The #P-hardness holds for 2-local Ising Hamiltonians, since the parametrized construction in Eq. (8.2.1) preserves 2-locality when $H$ is 2-local.

The exact oracle is unrealistic. A robust version of Lemma 8.2.1 must tolerate additive noise $\varepsilon$ in the oracle outputs. Paturi's amplification lemma controls how pointwise bounds on a polynomial propagate across an interval.

**Lemma 8.2.2** (Paturi [21]). *Let $P(x)$ be a polynomial of degree at most $M$ satisfying $|P(i)| \leq c$ for all integers $i \in \{0, 1, \ldots, M\}$. Then $|P(x)| \leq c \cdot 2^M$ for all $x \in [0, M]$.*

Paturi's lemma bounds the growth of a polynomial between its sample points: a polynomial bounded by $c$ at $M+1$ integer points can exceed $c$ by at most a factor $2^M$ on the interval. When applied to the difference between the exact and approximate reconstruction polynomials, it yields a controlled error on the interpolation interval. The oracle noise $\varepsilon$ propagates to $f$ as $|\tilde{f}(x_i) - f(x_i)| \leq 3\varepsilon$ (three oracle calls contribute), then to the polynomial samples as $|\tilde{P}(x_i) - P(x_i)| \leq 3\varepsilon \prod_k (\Delta_k + x_i/2)$. The product is at most $B^M$ where $B = \Delta_{\max} + M = \text{poly}(n)$, so each sample has error at most $3\varepsilon B^M$.

**Lemma 8.2.3** (Approximate degeneracy extraction [10]). *Under the same hypotheses as Lemma 8.2.1, but with an oracle $\mathcal{C}_\varepsilon$ satisfying $|\widetilde{A}_1(H) - A_1(H)| \leq \varepsilon$: for sufficiently small $\varepsilon \in O(2^{-poly(n)})$, all degeneracies $d_k$ can be computed exactly by $O(poly(n))$ calls to $\mathcal{C}_\varepsilon$.*

*Proof sketch.* The approximate polynomial $\tilde{P}$ is the Lagrange interpolant through the noisy values $(\tilde{P}(x_1), \ldots, \tilde{P}(x_M))$. Its difference $D = \tilde{P} - P$ is a polynomial of degree at most $M-1$ bounded by $3\varepsilon B^M$ at the sample points. By Paturi's lemma (Lemma 8.2.2), $|D(x)| \leq 3\varepsilon B^M \cdot 2^{M-1}$ on the interpolation interval. At the pole evaluation points $x^* = -2\Delta_k$, which lie outside the interval $[1, 2M-1]$, the error is bounded by the Lagrange basis amplification:

$$|D(x^*)| \leq 3\varepsilon B^M \cdot \Lambda_M(x^*),$$

where $\Lambda_M(x^*) = \sum_j \prod_{i \neq j} |x^* - x_i|/|x_j - x_i|$ is the Lebesgue function. For extrapolation outside the interval, $\Lambda_M(x^*)$ grows exponentially in $M$, but since $M = \text{poly}(n)$, the total amplification is $2^{\text{poly}(n)}$. Dividing by $\prod_{\ell \neq k} |\Delta_\ell - \Delta_k|$ (also at most $2^{\text{poly}(n)}$ for integer gaps) and multiplying by $N = 2^n$, the degeneracy error satisfies

$$|d_k - \tilde{d}_k| \leq 3\varepsilon \cdot 2^{\text{poly}(n)}.$$

For $\varepsilon = O(2^{-\text{poly}(n)})$ with a sufficiently large polynomial, this is less than $1/2$. Since degeneracies are positive integers, rounding $\tilde{d}_k$ to the nearest integer recovers $d_k$ exactly. □

The proof extends to probabilistic oracles. If $\mathcal{C}_\varepsilon$ succeeds with probability at least $3/4$, then $O(\text{poly}(n))$ queries produce enough correct sample points to reconstruct $P$ despite corrupted evaluations. The Berlekamp-Welch algorithm recovers a polynomial of degree $d$ from $k$ partially corrupted evaluations, provided at least $\max\{d+1, (k+d)/2\}$ evaluations are correct [20]. By the Chernoff bound, querying $k = O(\text{poly}(n))$ times ensures that at least $(k + M - 2)/2$ evaluations are correct with high probability. Combining this with Lemma 8.2.3:

**Theorem 8.2.4** (#P-hardness of $A_1$ estimation [10]). *Estimating $A_1(H)$ to additive accuracy $\varepsilon = O(2^{-poly(n)})$ is #P-hard, even for 2-local Ising Hamiltonians. The result holds for both deterministic and probabilistic estimation algorithms.*

For the running example ($M = 2$), the reconstruction polynomial $P(x) = (d_0/N)(1 + x/2) + (d_1/N)(x/2)$ is linear. Two evaluations determine $d_0$ and $d_1$ exactly, and the Lagrange interpolation is trivial: a line through two points. The #P-hardness arises from Hamiltonians with $M = O(n^2)$ levels, where the reconstruction polynomial has high degree and small errors amplify through the exponential Paturi factor. The error amplification from oracle noise to degeneracy error grows as $2^{O(M \log n)}$, a factor that the next section analyzes precisely.

## 8.3 The Intermediate Regime

The adiabatic algorithm requires $A_1$ to precision $O(2^{-n/2})$. NP-hardness holds at $1/\text{poly}(n)$ (Theorem 8.1.2), and #P-hardness holds at $2^{-\text{poly}(n)}$ (Theorem 8.2.4). The algorithmically relevant precision $2^{-n/2}$ sits strictly between these regimes. The paper identifies this gap explicitly: "these proof techniques based on polynomial interpolation do not allow us to conclude anything about the hardness of the approximation of $A_1(H)$ up to the additive error tolerated by the adiabatic algorithm" [10].

The results of this section are contributions of this thesis, addressing this open problem.

NP-hardness extends to $2^{-n/2}$ by monotonicity: an oracle at precision $2^{-n/2}$ is strictly more powerful than one at $1/\text{poly}(n)$ (since $2^{-n/2} < 1/\text{poly}(n)$ for large $n$), so it also solves 3-SAT. But #P-hardness does not extend upward: an oracle at precision $2^{-n/2}$ is *less* powerful than one at $2^{-\text{poly}(n)}$, and the interpolation technique that established the latter breaks down at the former. The following theorem makes this breakdown precise.

**Theorem 8.3.1** (Interpolation barrier). *The polynomial interpolation technique of section 8.2 requires oracle precision $\varepsilon = 2^{-n-O(M \log n)}$ to extract exact degeneracies, where $M = poly(n)$ is the number of distinct energy levels. At $\varepsilon = 2^{-n/2}$, the amplified error exceeds $1/2$ and rounding fails. The #P-hardness argument does not extend to precision $2^{-n/2}$.*

*Proof.* We trace the error propagation from oracle noise to degeneracy error through the construction of Lemma 8.2.1. Let $\varepsilon$ denote the oracle accuracy, and let $B = \Delta_{\max} + M = \mathrm{poly}(n)$ bound the denominator factors, where $\Delta_{\max}$ is the largest spectral gap.

**Sample-point error.** The approximate function values satisfy $|\tilde{f}(x_i) - f(x_i)| \le 3\varepsilon$. The approximate polynomial samples are $\tilde{P}(x_i) = \prod_k (\Delta_k + x_i/2)\,\tilde{f}(x_i)$, with error

$$|\tilde{P}(x_i) - P(x_i)| \le 3\varepsilon \prod_{k=0}^{M-1} \left(\Delta_k + \frac{x_i}{2}\right) \le 3\varepsilon\, B^M. \tag{8.3.1}$$

**Degeneracy error.** The approximate degeneracies are computed from Eq. (8.2.4) with $\tilde{P}$ in place of $P$. Since $\tilde{P}$ is the Lagrange interpolant through the noisy samples, its value at any point $x^*$ is $\tilde{P}(x^*) = \sum_j \tilde{P}(x_j) \prod_{i\neq j} (x^* - x_i)/(x_j - x_i)$. The error at $x^* = -2\Delta_k$ satisfies

$$|\tilde{P}(x^*) - P(x^*)| \le 3\varepsilon\, B^M \sum_{j=0}^{M-1} \prod_{i\neq j} \frac{|x^* - x_i|}{|x_j - x_i|} = 3\varepsilon\, B^M \cdot \Lambda_M(x^*), \tag{8.3.2}$$

where $\Lambda_M(x^*)$ is the Lebesgue function at $x^*$. For the odd-integer nodes $x_j = 2j + 1$ and evaluation point $x^* = -2\Delta_k \le 0$ (outside the interval $[1, 2M-1]$): each numerator factor $|x^* - x_i| = 2\Delta_k + 2i + 1 \le 2B + 1$. For the denominator, $\prod_{i\neq j} |x_j - x_i| = \prod_{i\neq j} 2|j - i| = 2^{M-1}\, j!\,(M-1-j)!$, since the nodes are equally spaced with spacing 2. The sum over $j$ evaluates to

$$\Lambda_M(x^*) \le \sum_{j=0}^{M-1} \frac{(2B+1)^{M-1}}{2^{M-1}\, j!\,(M-1-j)!} = \frac{(2B+1)^{M-1}}{(M-1)!}, \tag{8.3.3}$$

using the identity $\sum_j \binom{M-1}{j} = 2^{M-1}$. The denominator in Eq. (8.2.4) satisfies $\prod_{\ell\neq k} |\Delta_\ell - \Delta_k| \ge k!(M-1-k)!$ for integer gaps (since $|\Delta_\ell - \Delta_k| \ge |\ell - k|$), with minimum over $k$ at least $((M-1)/(2e))^{M-1}$ by Stirling's approximation. The total degeneracy error is therefore

$$|d_k - \tilde{d}_k| \le \frac{3\varepsilon\, N\, B^M\, (2B+1)^{M-1}}{(M-1)!\,((M-1)/(2e))^{M-1}}. \tag{8.3.4}$$

Since $B = \mathrm{poly}(n)$ and $M = \mathrm{poly}(n)$, the amplification factor is $2^{O(M \log n)}$.

**Rounding condition.** To extract exact degeneracies by rounding, we need $|d_k - \tilde{d}_k| < 1/2$. This requires

$$\varepsilon < \frac{1}{6N \cdot 2^{O(M \log n)}} = 2^{-n - O(M \log n)}. \tag{8.3.5}$$

**Evaluation at $\varepsilon = 2^{-n/2}$.** Set $\varepsilon = 2^{-n/2}$ and $M = n^c$ for some constant $c \ge 1$. The error bound from Eq. (8.3.4) evaluates to

$$|d_k - \tilde{d}_k| \le 3 \cdot 2^{-n/2} \cdot 2^n \cdot 2^{O(n^c \log n)} = 3 \cdot 2^{n/2 + O(n^c \log n)} \gg 1.$$

Even for $c = 1$ (the most favorable case $M = n$), the exponent $n/2 + \Omega(n \log n)$ diverges. The upper bound on the degeneracy error already exceeds $1/2$, so the rounding step cannot be guaranteed to succeed. □

The barrier is not an artifact of the paper's specific construction. Any scheme that extracts integer degeneracies by evaluating a polynomial outside its interpolation interval faces exponential amplification. The Lebesgue function $\Lambda_d(x^*)$ satisfies $\Lambda_d(x^*) \ge 2^{d-1}$ whenever $x^*$ lies at distance at least $|b - a|$ from the interpolation interval $[a, b]$, regardless of how the $d$ nodes are placed within $[a, b]$. No rearrangement of interpolation nodes, no alternative polynomial basis, and no change of variables can circumvent this. The same structural obstacle appears in quantum computational advantage proposals: the polynomial interpolation techniques used to prove hardness of boson sampling [22] and random circuit sampling [23] face analogous amplification barriers when extending hardness from exponentially small to moderate error regimes.

The interpolation barrier does not rule out #P-hardness at $2^{-n/2}$ by other means. A proof that avoids polynomial extrapolation entirely — using direct algebraic reductions or information-theoretic arguments — might succeed. The barrier identifies where new proof techniques are needed: the challenge is to establish counting hardness without extracting exact integers from approximate real evaluations.

What can be computed at precision $2^{-n/2}$? We analyze the problem in the query model, where each query to a diagonal oracle $O_H\colon |x\rangle\,|0\rangle \mapsto |x\rangle\,|E_x\rangle$ reveals one diagonal entry of $H_z$. This framework cleanly separates quantum and classical capabilities.

**Theorem 8.3.2** (Quantum algorithm for $A_1$)**.** *There exists a quantum algorithm that estimates $A_1(H_z)$ to additive precision $\varepsilon$ using*

$$O\left(\sqrt{N} + \frac{1}{\varepsilon\,\Delta_1}\right) \tag{8.3.6}$$

*quantum queries to the diagonal oracle $O_H$, where $\Delta_1 = E_1 - E_0$ is the spectral gap of $H_z$.*

*Proof.* The algorithm has two stages.

**Stage 1: Finding $E_0$.** The Hamiltonian $H_z$ is diagonal in the computational basis, so computing $E_x$ for a given $|x\rangle$ requires one query to $O_H$. Finding the minimum of $E_x$ over all $x \in \{0,1\}^n$ is an instance of quantum minimum finding [24], which succeeds with high probability in $O(\sqrt{N})$ queries.

**Stage 2: Amplitude estimation of $A_1$.** Define the function

$$g(x) = \begin{cases} \dfrac{1}{E_x - E_0} & \text{if } E_x \neq E_0, \\ 0 & \text{if } E_x = E_0. \end{cases}$$

The spectral parameter is the mean $A_1 = (1/N)\sum_x g(x)$. Since the eigenvalues lie in $[0,1]$, the values of $g$ on non-ground states are in $[1, 1/\Delta_1]$. Rescaling to $h(x) = \Delta_1 \cdot g(x)$ yields $h(x) \in [0,1]$, and $A_1 = \mu_h/\Delta_1$ where $\mu_h = (1/N)\sum_x h(x)$.

Construct a quantum oracle $U_h$ acting as $U_h\colon\ |x\rangle\,|0\rangle \mapsto |x\rangle\,(\sqrt{1-h(x)}\,|0\rangle + \sqrt{h(x)}\,|1\rangle)$. The implementation queries $O_H$ once to obtain $E_x$, performs classical arithmetic on an ancilla to compute $h(x) = \Delta_1/(E_x - E_0)$ (or 0 for ground states), executes a controlled rotation $R_y(2\arcsin\sqrt{h(x)})$ on a flag qubit, and uncomputes the ancilla. Each application uses $O(1)$ queries to $O_H$ and $O(\mathrm{poly}(n))$ auxiliary gates.

Preparing the uniform superposition $|+\rangle^{\otimes n}$ and applying $U_h$, the probability of measuring the flag qubit in $|1\rangle$ is

$$p = \frac{1}{N}\sum_x h(x) = \mu_h.$$

Amplitude estimation [25] estimates $p$ to additive precision $\delta$ using $O(1/\delta)$ applications of $U_h$ and its inverse. Setting $\delta = \varepsilon\,\Delta_1$ ensures $|A_1 - \tilde{A}_1| = |\mu_h - \tilde{\mu}_h|/\Delta_1 \leq \varepsilon$. The number of $U_h$ applications is $O(1/(\varepsilon\,\Delta_1))$.

Combining both stages: $O(\sqrt{N})$ queries for Stage 1 and $O(1/(\varepsilon\,\Delta_1))$ queries for Stage 2, giving the total in Eq. (8.3.6). For $\varepsilon = 2^{-n/2}$ and $\Delta_1 = 1/\mathrm{poly}(n)$: $O(2^{n/2} + 2^{n/2}\,\mathrm{poly}(n)) = O(2^{n/2}\,\mathrm{poly}(n))$. □

**Theorem 8.3.3** (Classical lower bound for $A_1$ estimation)**.** *Any classical randomized algorithm estimating $A_1(H_z)$ to additive precision $\varepsilon$ in the query model requires $\Omega(1/\varepsilon^2)$ queries in the worst case.*

*Proof.* We construct an adversarial pair of instances that are indistinguishable without sufficiently many queries.

**Instance construction.** Fix $t = \lceil \varepsilon N \rceil$. Instance $H_0$ has a hidden set $S \subseteq \{0,1\}^n$ with $|S| = N/2$, and eigenvalues $E_x = 0$ for $x \in S$, $E_x = 1$ otherwise. Instance $H_1$ has $|S'| = N/2 + t$ ground states. The spectral parameters are $A_1(H_0) = 1/2$ and $A_1(H_1) = (N/2 - t)/N = 1/2 - t/N$, differing by $t/N \geq \varepsilon$. An algorithm estimating $A_1$ to precision $\varepsilon/2$ must distinguish the two instances.

**Information-theoretic bound.** A classical query at string $x$ reveals $E_x \in \{0,1\}$, equivalent to learning whether $x \in S$. Under a uniform prior on $S$ (or $S'$), successive queries follow a hypergeometric sampling model. For the $j$-th query ($j \leq q \ll N$), the conditional per-query KL divergence between the two hypotheses is

$$D_j = O\left(\frac{t^2}{(N-j)^2}\right) = O\left(\frac{t^2}{N^2}\right)$$

when $q \leq N/2$. By the chain rule for KL divergence, the total information from $q$ adaptive queries is

$$D_{\mathrm{KL}}^{(q)} \leq \sum_{j=1}^{q} D_j \leq q \cdot O\left(\frac{t^2}{N^2}\right).$$

By Le Cam's two-point method [26], reliable hypothesis testing requires $D_{\mathrm{KL}}^{(q)} \geq \Omega(1)$ (via Pinsker's inequality: total variation distance $\leq \sqrt{D_{\mathrm{KL}}/2}$, and distinguishing requires total variation $\Omega(1)$). Therefore

$$q \geq \Omega\left(\frac{N^2}{t^2}\right) = \Omega\left(\frac{1}{\varepsilon^2}\right).$$

At $\varepsilon = 2^{-n/2}$: $q \geq \Omega(2^n)$. □

**Corollary 8.3.4** (Quadratic quantum-classical separation)**.** *In the query model, estimating $A_1(H_z)$ to precision $\varepsilon = 2^{-n/2}$ exhibits a quadratic quantum-classical separation: quantum complexity $O(2^{n/2}\,\mathrm{poly}(n))$ versus classical complexity $\Omega(2^n)$.*

*Proof.* The upper bound is Theorem 8.3.2 with $\Delta_1 = 1$ for the adversarial instance (or $\Delta_1 = 1/\mathrm{poly}(n)$ in general). The lower bound is Theorem 8.3.3. The separation ratio is $\Omega(2^{n/2}/\mathrm{poly}(n))$, matching Grover's quadratic speedup for unstructured search. □

The quantum upper bound in Theorem 8.3.2 is tight. For $M = 2$ instances with $\Delta_1 = 1$, estimating $A_1 = (N - d_0)/N$ to precision $\varepsilon$ is equivalent to estimating the fraction $d_0/N$ to precision $\varepsilon$, which is an instance of approximate counting. The Grover iterate $G = (2\,|+\rangle\langle+| - I)(I - 2\Pi_S)$, where $\Pi_S$ projects onto the $d_0$ ground states, has eigenphases $\pm 2\theta$ with $\sin^2\theta = d_0/N$. For $d_0 \approx N/2$, the derivative $dp/d\theta = \sin 2\theta = 1$, so precision $\varepsilon$ in $A_1$ requires precision $\varepsilon$ in $\theta$. The Heisenberg limit for quantum phase estimation [27] — the quantum Cramér-Rao inequality with Fisher information $F_Q \leq 4T^2$ — gives $T \geq 1/(2\varepsilon)$ applications of $G$, each costing $O(1)$ oracle queries. Combined with the upper bound: the quantum query complexity at precision $\varepsilon = 2^{-n/2}$ is $\Theta(2^{n/2})$.

For Grover search with $N = 4$ ($n = 2$), the quantum algorithm uses $O(\sqrt{4} + 2) = O(4)$ queries at precision $\varepsilon = 1/2$, while the classical lower bound gives $\Omega(4)$. The separation is trivial at this scale but grows as $\Omega(2^{n/2}/\mathrm{poly}(n))$ with $n$.

Two complementary frameworks apply: computational complexity for the problem of estimating $A_1$ given an explicit Hamiltonian description, and query complexity for the problem given oracle access to the diagonal entries.

In the computational model with an explicit Hamiltonian description, the complexity landscape across precision regimes is:

| Precision $\varepsilon$ | Hardness | Source |
|---|---|---|
| $1/\mathrm{poly}(n)$ | NP-hard | Theorem 8.1.2 |
| $2^{-n/2}$ | NP-hard | monotonicity |
| $2^{-\mathrm{poly}(n)}$ | #P-hard | Theorem 8.2.4 |

In the query model with a diagonal oracle at the algorithmically relevant precision $\varepsilon = 2^{-n/2}$:

| Model | Complexity | Source |
|---|---|---|
| Quantum | $O(2^{n/2} \cdot \mathrm{poly}(n))$ | Theorem 8.3.2 |
| Classical | $\Omega(2^n)$ | Theorem 8.3.3 |

The precision $2^{-n/2}$ coincides with the algorithmic requirement: the adiabatic schedule needs $A_1$ to precision $O(\sqrt{d_0/N})$, which is $O(2^{-n/2})$ in the worst case $d_0 = O(1)$. It is also the interpolation barrier: the proof technique that establishes #P-hardness breaks exactly at this threshold (Theorem 8.3.1), while NP-hardness extends by monotonicity. And it marks a query complexity transition: at $2^{-n/2}$, the quantum algorithm achieves $O(2^{n/2})$ queries while classical sampling requires $\Omega(2^n)$, a Grover-type quadratic gap.

Independent of the query-complexity analysis, classical sampling provides direct evidence for the hardness of $A_1$ estimation at the algorithmic precision. Given a procedure that samples eigenvalues $E_x$ according to the distribution $\{d_k/N\}$, estimating the mean $A_1 = \mathbb{E}[1/(E_x - E_0)]$ to precision $\delta_s$ requires $O(1/\delta_s^2) = \widetilde{O}(2^n/d_0)$ samples by Chebyshev's inequality [28]. This matches the formal $\Omega(2^n)$ lower bound of Theorem 8.3.3 up to logarithmic factors, providing a consistency check between the query-complexity result and concrete sampling algorithms.

The results of this chapter create a tension. The adiabatic algorithm of Theorem 7.3.1 achieves the Grover speedup $\widetilde{O}(\sqrt{N/d_0})$, matching the lower bound for unstructured search. But the algorithm's schedule requires a spectral parameter whose computation is NP-hard, even at a precision far coarser than what the algorithm needs. In the circuit model, Grover's algorithm achieves the same speedup without pre-computing any spectral parameter: oracle queries gather information adaptively during execution. The adiabatic framework demands the schedule be fixed before evolution begins.

This asymmetry raises a precise question. Does the information cost of the adiabatic approach represent a fundamental limitation, or can it be circumvented? What runtime is achievable by an adiabatic algorithm that knows nothing about the problem Hamiltonian beyond its dimension? The next chapter formalizes this as an information-runtime tradeoff, proving a separation theorem for uninformed schedules and exploring whether adaptive measurements can bypass the classical pre-computation barrier.

# Chapter 9

# Information Gap

# Chapter 10

# Formalization

# Chapter 11

# Conclusion

# Bibliography


[1] Jeremie Roland and Nicolas J. Cerf. Quantum search by local adiabatic evolution. *Physical Review A*, 65 (4):042308, 2002. doi:10.1103/PhysRevA.65.042308.

[2] Edward Farhi, Jeffrey Goldstone, Sam Gutmann, and Daniel Nagaj. How to make the quantum adiabatic algorithm fail. *International Journal of Quantum Information*, 6(03):503–516, 2008. doi:10.1142/S021974990800358X.

[3] Marko Žnidarič and Martin Horvat. Exponential complexity of an adiabatic algorithm for an NP-complete problem. *Physical Review A*, 73:022329, 2006. doi:10.1103/PhysRevA.73.022329.

[4] Itay Hen. Continuous-time quantum algorithms for unstructured problems. *Journal of Physics A: Mathematical and Theoretical*, 47(4):045305, 2014. doi:10.1088/1751-8113/47/4/045305.

[5] F. Barahona. On the computational complexity of Ising spin glass models. *Journal of Physics A: Mathematical and General*, 15(10):3241, 1982. doi:10.1088/0305-4470/15/10/028.

[6] Andrew Lucas. Ising formulations of many NP problems. *Frontiers in Physics*, 2:5, 2014. doi:10.3389/fphy.2014.00005.

[7] Lov K. Grover. A fast quantum mechanical algorithm for database search. In *Proceedings of the 28th Annual ACM Symposium on Theory of Computing*, pages 212–219, 1996. doi:10.1145/237814.237866.

[8] Charles H. Bennett, Ethan Bernstein, Gilles Brassard, and Umesh Vazirani. Strengths and weaknesses of quantum computing. *SIAM Journal on Computing*, 26(5):1510–1523, 1997. doi:10.1137/S0097539796300933.

[9] Tameem Albash and Daniel A. Lidar. Adiabatic quantum computation. *Reviews of Modern Physics*, 90: 015002, 2018. doi:10.1103/RevModPhys.90.015002.

[10] Arthur Braida, Shantanav Chakraborty, Leonardo Novo, and Jérémie Roland. Unstructured adiabatic quantum optimization: Optimality with limitations. *arXiv preprint arXiv:2411.05736*, 2024.

[11] Gene H. Golub. Some modified matrix eigenvalue problems. *SIAM Review*, 15(2):318–334, 1973. doi:10.1137/1015032.

[12] Shantanav Chakraborty, Leonardo Novo, and Jérémie Roland. Optimality of spatial search via continuous-time quantum walks. *Physical Review A*, 102:032214, 2020. doi:10.1103/PhysRevA.102.032214.

[13] Jack Sherman and Winifred J. Morrison. Adjustment of an inverse matrix corresponding to a change in one element of a given matrix. *The Annals of Mathematical Statistics*, 21(1):124–127, 1950. doi:10.1214/aoms/1177729893.

[14] Sergio Boixo, Emanuel Knill, and Rolando Somma. Eigenpath traversal by phase randomization. *Quantum Information and Computation*, 9(9):833–855, 2009.

[15] Joseph Cunningham and Jérémie Roland. Eigenpath traversal by Poisson-distributed phase randomisation. In *19th Conference on the Theory of Quantum Computation, Communication and Cryptography (TQC 2024)*, pages 7:1–7:20, 2024. doi:10.4230/LIPIcs.TQC.2024.7.

[16] Julia Kempe, Alexei Kitaev, and Oded Regev. The complexity of the local Hamiltonian problem. *SIAM Journal on Computing*, 35(5):1070–1097, 2006. doi:10.1137/S0097539704445226.

[17] M.R. Garey, D.S. Johnson, and L. Stockmeyer. Some simplified NP-complete graph problems. *Theoretical Computer Science*, 1(3):237–267, 1976. doi:10.1016/0304-3975(76)90059-1.

[18] Leslie G. Valiant. The complexity of enumeration and reliability problems. *SIAM Journal on Computing*, 8(3):410–421, 1979. doi:10.1137/0208032.

[19] George M. Phillips. *Interpolation and Approximation by Polynomials*, volume 14. Springer Science & Business Media, 2003. doi:10.1007/b97417.

[20] Ramis Movassagh. The hardness of random quantum circuits. *Nature Physics*, 19(11):1719–1724, 2023. doi:10.1038/s41567-023-02131-2.

[21] Ramamohan Paturi. On the degree of polynomials that approximate symmetric Boolean functions. In *Proceedings of the 24th Annual ACM Symposium on Theory of Computing*, pages 468–474, 1992. doi:10.1145/129712.129758.

[22] Scott Aaronson and Alex Arkhipov. The computational complexity of linear optics. In *Proceedings of the 43rd Annual ACM Symposium on Theory of Computing*, pages 333–342, 2011. doi:10.1145/1993636.1993682.

[23] Adam Bouland, Bill Fefferman, Chinmay Nirkhe, and Umesh Vazirani. On the complexity and verification of quantum random circuit sampling. *Nature Physics*, 15(2):159–163, 2019. doi:10.1038/s41567-018-0318-2.

[24] Christoph Dürr and Peter Høyer. A quantum algorithm for finding the minimum. *arXiv preprint quant-ph/9607014*, 1996.

[25] Gilles Brassard, Peter Høyer, Michele Mosca, and Alain Tapp. Quantum amplitude amplification and estimation. *Contemporary Mathematics*, 305:53–74, 2002. doi:10.1090/conm/305/05215.

[26] Lucien Le Cam. Convergence of estimates under dimensionality restrictions. *The Annals of Statistics*, 1 (1):38–53, 1973. doi:10.1214/aos/1176342150.

[27] Vittorio Giovannetti, Seth Lloyd, and Lorenzo Maccone. Quantum metrology. *Physical Review Letters*, 96: 010401, 2006. doi:10.1103/PhysRevLett.96.010401.

[28] Leonid Gurvits. On the complexity of mixed discriminants and related problems. In *Proceedings of the 30th International Conference on Mathematical Foundations of Computer Science*, pages 447–458, 2005. doi:10.1007/11549345_39.